

# SKBF TECHNICAL KBS REPORT

**84-04**

## ANALYSIS OF SOME LABORATORY TRACER RUNS IN NATURAL FISSURES

Luis Moreno  
Ivars Neretnieks  
The Royal Institute of Technology  
Department of Chemical Engineering

Trygve E Eriksen  
Royal Institute of Technology  
Department of Nuclear Chemistry

Stockholm, Sweden 1984-03-15

ANALYSIS OF SOME LABORATORY TRACER RUNS  
IN NATURAL FISSURES

Luis Moreno  
Ivars Neretnieks  
The Royal Institute of Technology  
Department of Chemical Engineering

Trygve Eriksen  
The Royal Institute of Technology  
Department of Nuclear Chemistry

Stockholm, Sweden 1984-03-15

This report concerns a study which was conducted for SKBF/KBS. The conclusions and viewpoints presented in the report are those of the author(s) and do not necessarily coincide with those of the client.

A list of other reports published in this series during 1984 is attached at the end of this report. Information on KBS technical reports from 1977-1978 (TR 121), 1979 (TR 79-28), 1980 (TR 80-26), 1981 (TR 81-17), 1982 (TR 82-28) and 1983 (TR 83-77) is available through SKBF/KBS.



ANALYSIS OF SOME LABORATORY TRACER RUNS IN NATURAL FISSURES

1984-03-15

Luis Moreno  
Ivars Neretnieks  
Department of  
Chemical Engineering

Trygve Eriksen  
Department of  
Nuclear Chemistry

## CONTENTS

	Page
Summary	
1. Introduction	1
2. The experimental data	2
3. Description of the model	3
4. The governing equations	5
4.1 Hydrodynamic dispersion-diffusion model	5
4.2 Channeling dispersion-diffusion model	8
4.3 Breakthrough curve for the effluent	10
4.4 Determination of the parameters	11
5. Fit of the experimental data	12
6. Comparison between the two models for prediction purposes	16
7. Discussion	18
8. Conclusions	19
Notation	20
References	21
Tables	
Figures	

## SUMMARY

Tracer tests in natural fissures performed in the laboratory are analysed by means of fitting two different models. In the experiments, sorbing and non-sorbing tracers were injected into a natural fissure running parallel to the axis of a drill core. The models take into account advection, diffusion into the rock matrix, sorption onto the rock surface and dispersion. For the last mechanism, one of the models considers hydrodynamic dispersion while the other model assumes channeling dispersion. The models take into account time delays in the inlet and outlet channels.

The dispersion characteristics and water residence time were determined from the experiments with non-sorbing tracers. Surface and volume sorption coefficients and data on diffusion into the rock matrix were determined for the sorbing tracers. The results are compared with values independently determined in the laboratory. Good agreement was obtained using either model.

When these models are used for prediction of tracer transport over larger distances, the results will depend on the model. The model with channeling dispersion will show a greater dispersion than the model with hydrodynamic dispersion.

## 1.0 Introduction

The final disposal of radioactive wastes from nuclear power plants has been studied in many countries. In Sweden, crystalline rock has been selected as the most suitable bedrock in which to build a repository. If a canister is broken, radionuclides will be carried by the water flowing in the bedrock. The radionuclides may interact with the rock by means of sorption onto the surface of the fissures and microfissures and by diffusion into the rock matrix and sorption onto the surfaces of the inner microfissures.

The sorption of radionuclides on the rock and the diffusion into it have been studied in laboratory experiments. The transport through fissures in the rock has been studied both in the laboratory and in in situ experiments.

The aim of this study is to test the capability of two models to predict the transport of strontium through a single fissure using data from experiments carried out in the laboratory. Velocity variations are modelled by hydrodynamic dispersion in one model and by channeling dispersion in the other model. The influence of the selected model, when the results from these tests are used to predict breakthrough curves for longer migration distances, is also studied.

## 2.0 The experimental data

Two granitic drill cores, taken from the Stripa mine, were used in the experiments. Each drill core had a natural fissure running parallel to the axis.

The dimensions of drill cores were: core A - 18.5 cm in height and 10.0 cm in diameter, core B - 27.0 cm in height and 10.0 cm in diameter.

Figure 1 shows the experimental set-up. Tracers were injected into the upper channel in core A and into the lower channel in core B. The outlet channel was simultaneously flushed with water to reduce the delay time due to the channel volume. The experimental technique is described in some detail by Neretnieks et al (1982).

The tritiated water, iodide, bromide and lignosulphonate ions were selected as non-sorbing tracers. Strontium was used as a sorbing ion. The experiments were performed at the department of Nuclear Chemistry by Eriksen and co-workers.

The porosity of Stripa granite and diffusivity of the iodide tracer and the tritiated water have been determined by Skagius and Neretnieks (1982, 1983). The surface and volume distribution coefficients and diffusivity of strontium have also been determined (Skagius et al., 1982 and Skagius and Neretnieks, 1983).



### 3.0 Description of the model

The transport of a species carried by a fluid flowing in a fissure in rock is influenced by:

- o molecular diffusion in the liquid
- o variations in fluid velocity in the fissure
- o velocity variations between channels in the fissure
- o chemical or physical interactions with the solid material.

The models describe the tracer transport as taking place through a parallel-walled fissure. The tracers penetrate the matrix by molecular diffusion and they may be sorbed onto the fissure walls and onto microfissure surfaces within the rock matrix. The transversal dispersion in the fissure is assumed to be negligible.

The water residence time in the inlet channel as well as in the outlet channel is important compared with the residence time in the fissure proper. The channel used to distribute the tracer along the fissure inlet had a volume of 1.1 ml and the volume of the outlet channel was about the same.

The water residence time in the inlet channel depends on the flow of tracer injection. The ratio of the flow of flushing water to the flow through the fissure determines the water residence time in the outlet channel. If the overall flow through the fissure is thought of being the sum of the flows following several distinct pathways, each pathway will have a different time delay in the inlet channel and in the outlet channel. The pathway closest to the inlet will have the least time delay in the inlet and the greatest in the outlet. Dispersion for each pathway in the inlet and outlet channels is assumed to be negligible. Continuous flushing of the outlet channel makes the residence time there less than in the inlet channel.

Spreading in the effluent will be also caused by the variation in residence time for the different pathways. Two models are used to describe the transport through a given pathway in the fissure. The first model assumes that tracers flow in a parallel-walled fissure with spreading due to hydrodynamic Fickian type dispersion. In the second model, it is assumed that the fissure consists of parallel unconnected channels, the channel widths having a lognormal distribution. This causes the velocities to be different in different channels. The hydrodynamic dispersion in each channel is assumed to be negligible i.e. in this case the "dispersion" is entirely due to the variation in flow velocity through the different channels. The models are shown graphically in figure 2.

#### 4.0 The governing equations

The flow through the inlet channel, fissure and outlet channel is divided into various pathways as shown in figure 2a. Each pathway has a different time delay. The tracer movement in the fissure proper is studied considering two different models:

- o hydrodynamic dispersion-diffusion model
- o channeling dispersion-diffusion model

In the first model, the spreading of the tracer in the fissure is taken into account by means of hydrodynamic dispersion which is modelled as Fickian dispersion. The other model postulates that the tracer will be carried different distances in a given time due to the velocity variations between the channels. The velocity variations are due to the differences in channel width and/or flow resistance.

#### 4.1 Hydrodynamic dispersion-diffusion model

The model considers the transport of contaminants in a fluid that flows through a thin fracture in a water-saturated porous rock. The tracers penetrate the rock matrix by molecular diffusion and they may be sorbed onto the fracture surface and within the rock matrix.

The following processes will be considered:

- o advective transport along the fracture
- o longitudinal mechanical dispersion in the fracture
- o molecular diffusion from the fracture into the rock matrix
- o sorption onto the surface of the fracture
- o sorption within the rock matrix.

Assuming a linear isotherm for the surface sorption, the differential equation for the transport of a tracer in the fissure may be written in the following way:

$$\frac{\partial C_f}{\partial t} - \frac{D_L}{R_a} \frac{\partial^2 C_f}{\partial x^2} + \frac{U_f}{R_a} \frac{\partial C_f}{\partial x} - \frac{2}{\delta} \frac{D_e}{R_a} \frac{\partial C_p}{\partial z} \Big|_{z=0} = 0 \quad (1)$$

where  $R_a$  is the surface retardation coefficient defined as:

$$R_a = 1 + \frac{2}{\delta} K_a \quad (2)$$

The differential equation for the porous matrix is:

$$\frac{\partial C_p}{\partial t} - \frac{D_e}{K_d \rho_p} \frac{\partial^2 C_p}{\partial z^2} = 0 \quad (3)$$

$$0 < z < \infty$$

$K_d$  is the bulk equilibrium constant; it is based on the mass of microfissured solid and includes the nuclide which is on the solid as well as in the water in the microfissures.  $K_d$  is related to the equilibrium constant based on the mass of the solid proper,  $K'_d$ , by:

$$K_d \rho_p = \epsilon_p + K'_d \rho_p \quad (4)$$

$K_d \rho_p$  is usually the entity determined in sorption measurements. The difference between  $K'_d \rho_p$  and  $K_d \rho_p$  is negligible for sorbing tracers on low-porosity materials such as crystalline rock.  $K'_d \rho_p \gg \epsilon_p$  for such systems.

The system of equations (1) and (3) was solved by Tang et al. (1981) including radioactive decay for the initial and boundary conditions in the experiments.

The tracer concentration in the outlet for non-radioactive tracer may be written as:

$$\frac{C(t)}{C_0} = \frac{2}{\sqrt{\pi}} \exp\left(\frac{Pe}{2}\right) \int_{\lambda}^{\infty} \exp\left(-\xi^2 - \frac{Pe^2}{16\xi}\right) \cdot \operatorname{erfc}\left(\frac{\frac{Pe t_0}{8 A \xi^2}}{\sqrt{t - \frac{Pe t_0}{4 \xi^2}}}\right) d\xi \quad (5)$$

where:

$$\lambda = \left(\frac{Pe t_0}{4 t}\right)^{1/2} \quad (6)$$

$$Pe = \frac{U_f x}{D_L} \quad (7)$$

$$t_0 = R_a \frac{x}{U_f} = R_a t_w$$

$$A = \frac{\delta R_a}{2 (D_e K_d \rho_p)^{1/2}} \quad (9)$$

#### 4.2 Channeling dispersion-diffusion model.

The dispersion that occurs in the direction of the flow is accounted for by means of channeling dispersion. The velocity differences in the channels will carry a tracer different distances over a given time. The tracer will be dispersed.

The transport of the tracers takes place through a fracture, in which parallel channels with different widths exist. This is shown in figure 2c. It is assumed that the fissure widths have a lognormal distribution and the interconnection between the different channels is negligible. The hydrodynamic dispersion in each single channel is also assumed to be negligible compared to the effects of channeling.

The model includes the following mechanisms:

- o advective transport along the fissure
- o channeling dispersion
- o sorption onto the surface of the channels
- o diffusion into the rock matrix
- o sorption within the rock matrix.

For a tracer flowing through a fissure with negligible longitudinal dispersion, the equation for the concentration in the fissure is:

$$R_a \frac{\partial C_f}{\partial t} + U_f \frac{\partial C_f}{\partial x} - D_e \frac{\partial^2 C_p}{\partial z^2} \Big|_{z=0} = 0 \quad 0 < x < \infty \quad (10)$$

The equation for the diffusion into the rock matrix is given as before by equation (3).

The solution for equations (10) and (3) is found in the literature (Carslaw and Jaeger, 1959):

$$\frac{C_f}{C_0} = \operatorname{erfc} \left( \frac{B t_w}{\delta (t-t_0)^{1/2}} \right) \quad (11)$$

where:

$$t_0 = R_a \cdot t_w \quad (12)$$

$$B = (D_e K_d \rho_p)^{1/2} \quad (13)$$

If in each pathway separate channels exist with different fissure widths,  $\delta$ , the fluid will have different velocities in the different channels when flowing through the fissure. In this case  $R_a$  will be different for the different channels. The constant entity is  $K_a$ , the surface equilibrium coefficient. If the breakthrough curve for each channel in the actual pathway is given as  $C_f(\delta, t)$  then the concentration of the mixed effluent from the all channels in the pathway is (Neretnieks et al., 1982):

$$\frac{C(t)}{C_0} = \frac{\int_0^{\infty} f(\delta) Q(\delta) C_f(\delta, t) d\delta}{\int_0^{\infty} f(\delta) Q(\delta) d\delta} \quad (14)$$

In a parallel-walled channel of width  $\delta$ , the flow rate for laminar flow is proportional to the fissure width cubed. Snow (1970), studying the fissure frequencies for consolidated rock, found that the fissure widths have a lognormal distribution. The density function has the form:

$$f(\delta) = \frac{1}{\sigma \sqrt{2\pi}} \frac{1}{\delta} \exp \left( - \frac{[\ln(\delta/\mu)]^2}{2 \sigma^2} \right) \quad (15)$$

### 4.3 Breakthrough curve for the effluent

To account for the influence of the finite volumes of the inlet and outlet channels, time delays must be considered. Each pathway may be characterized by the dimensionless distance to the inlet,  $\xi$ . The time delay for a pathway may be written as:

$$t_D = t_{D1}(\xi, q) + t_{D2}(\xi, q, f) \quad (16)$$

where  $q$  is the water flow rate through the fissure and  $f$  is the ratio of the flushing flow to the flow  $q$ . The breakthrough curve at the outlet for a given pathway is:

$$C = C' (t - t_D) = C(\xi, t) \quad (17)$$

and the concentration of the mixed effluent from all the pathways is:

$$C(t) = \int_0^1 C(\xi, t) d\xi \quad (18)$$



#### 4.4 Determination of the parameters

The concentration of the effluent from all the pathways for the hydrodynamic dispersion-diffusion model may be written as:

$$\frac{C(t)}{C_0} = f (Pe, t_w, K_a, A, t) \quad (19)$$

For the channeling dispersion-diffusion model the concentration of the effluent becomes:

$$\frac{C(t)}{C_0} = f (\sigma, \bar{t}_w, K_a, B, t) \quad (20)$$

The determination of the parameter was done by means of a non-linear least squares fitting.

The runs with non-sorbing tracers were used for the determination of the hydraulic properties. These properties (Peclet number and water residence time for the hydrodynamic dispersion model and standard deviation of the logarithmic fissure width distribution and mean residence time for the channeling model) are used in the runs with the sorbing tracer to determine the other parameters. When the water residence time  $t_w$  (or equivalent fissure width) is known from the non-sorbing tracer runs, the surface equilibrium coefficient  $K_a$  and the product  $D_e \cdot K_d \cdot \rho_p$  are obtained from the sorbing tracer fits.

## 5.0 Fit of the experimental data

The modelling considers the existence of various pathways with different time delays. These time delays are calculated considering that the inlets for the tracer and the flushing water are on the same side of respective channels and that the outlet is on the opposite side of the inlet.

First, the experimental data was fitted using the hydrodynamic dispersion-diffusion model. For the tracer tests with non-sorbing substances, the determination of the parameter which takes into account the interaction with the rock matrix, the A-parameter, cannot be determined with any accuracy. The reason for this is the short tracer residence time, which results in a small interaction with the matrix. The water residence times were in the range 2-10 minutes. In the runs with non-sorbing tracer, the A-parameter was calculated assuming a value of  $D_e = 0.1 \cdot 10^{-12} \text{ m}^2/\text{s}$ . This value of the effective diffusivity has a very small impact on the breakthrough curve compared to when  $D_e = 0$ . Values for iodide and tritiated water were determined by Skagius and Neretnieks (1982) for pieces of granite. These values are in the range 0.07 to  $0.18 \cdot 10^{-12} \text{ m}^2/\text{s}$ . The effective diffusion coefficient for the lignosulfonate ion is assumed to be of the same order of magnitude or less than the iodide and tritiated water because this molecule is very large. A large molecule would have low access to the micropores of the rock matrix. The surface sorption coefficient is  $K_a = 0$  for a non-sorbing tracer.

The other parameters (Peclet number and water residence time in the fissure) are determined by means of a data fitting. From these values, the dispersion coefficient and the average fissure width are calculated. The results are shown in tables 1-2 and figures 3-11. For core A the average Peclet number was about 20 and the fissure width 0.14 mm. For core B these values were 15.0 and 0.13 mm respectively.

For the runs with sorbing tracer, the values of the Peclet number and fissure width determined in the runs with the non-sorbing tracers are used. The tracer residence time  $t_0$  and the parameter which takes into account the interaction with the rock matrix are determined by a data fitting. The inlet or reference concentration may be obtained directly from the experimental data, or may be assumed to be unknown and determined in the fit. Both fits, assuming a known reference concentration and assuming it to be unknown, are shown in figure 12. When the "known" reference concentration is used the fit is poor. For this reason the reference concentration was included in the fitting process. The results are shown in table 3 and the corresponding curves are shown in figures 13-18. The figures show the breakthrough curves for  $C/C_0$ , where  $C_0$  is the reference concentration determined by the fit. The reference concentration determined in the experiment is shown in table 3.

The surface sorption coefficient was about  $15.0 \cdot 10^{-5}$  m for core A and about  $8.6 \cdot 10^{-5}$  m for core B. The value determined in the laboratory (Skagius et al., 1982) is  $6.6 \cdot 10^{-5}$  m. From the value of the A-parameter it is only possible to determine the product ( $D_e \cdot K_d \cdot \rho_p$ ). In core A it was about  $2.1 \cdot 10^{-10}$  m<sup>2</sup>/s while it was about  $0.42 \cdot 10^{-10}$  m<sup>2</sup>/s in core B. The values determined in the laboratory were  $2.4 \cdot 10^{-12}$  m<sup>2</sup>/s for sawn pieces of granite and  $3.5 \cdot 10^{-12}$  m<sup>2</sup>/s when these values were determined using crushed granite particles, 5 mm in diameter. The sawn and crushed pieces had no coating material.

The channeling dispersion-diffusion model was used only to evaluate the experiments on core A both for the non-sorbing substance (NaLS) and sorbing substance (strontium). In the runs with the non-sorbing tracer NaLS, the A-parameter was calculated using a value of  $0.1 \cdot 10^{-12} \text{ m}^2/\text{s}$  for the effective diffusivity of the lignosulphonate ion. The other parameters were calculated by means of a fitting process (mean water residence time and standard deviation of the logarithm of the fissure width). The results for the non-sorbing substance are shown in table 4. The mean fissure width was 0.14 mm. This same value was obtained when the hydrodynamic dispersion model was used to fit these data. The mean standard deviation for the logarithm of the fissure width was  $\sigma = 0.155$  for these experiments.

To compare the standard deviation of the logarithmic fissure width distribution with the Peclet number, a theoretical relationship is determined. The breakthrough curve, for a tracer test with a step function in the injection at the inlet, is calculated as a function of the standard deviation of the logarithmic fissure width distribution,  $\sigma$ . Then the Peclet number is determined from the first and second moments of the breakthrough curve as (Levenspiel, 1972):

$$\frac{2}{\text{Pe}} = \frac{\Delta^2}{t'^2} \quad (21)$$

where for a step function injection:

$$t' = \int_0^{\infty} \frac{C(\infty) - C(\theta)}{C(\infty)} d\theta \quad (22)$$

$$\Delta^2 = 2 \int_0^{\infty} \theta \frac{[C(\infty) - C(\theta)]}{C(\infty)} d\theta - t'^2 \quad (23)$$

It is possible to find an analytical expression between Pe and  $\sigma$  (Neretnieks, 1983):

$$\frac{2}{Pe} = \exp(4\sigma^2) - 1 \quad (24)$$

The relation so obtained is shown in figure 19.

The values determined for the Peclet number and for the standard deviation of the logarithmic fissure width distribution, in the fits of the experimental runs, are also shown in figure 19. The differences are possibly due to the spreading caused by the different time delays of the pathways in the inlet and outlet zones. This spreading does not correspond to a random process. If the breakthrough curves are studied considering only the dispersion in the fissure, the agreement between Pe and  $\sigma$  is very good.

The runs of the sorbing tracer strontium were also fitted by means of the channeling dispersion-diffusion model. The water residence time was calculated from the previously determined fissure width and the flow rate. The standard deviation of the logarithmic fissure width distribution was also assumed to be known from the runs with lignosulphonate. A  $\sigma$ -value of 0.153 was used. This value corresponds to a Peclet number of 20. The results are shown in table 5. A comparison with the results using the hydrodynamic dispersion model is also shown. In the model the same fissure width and a Peclet number of 20 was used.

When the same hydraulic properties for the fissure are used, the channeling dispersion model needs a lower interaction with the rock matrix to fit the experimental data. This lower interaction compensates for the higher spreading produced by the surface sorption. The surface sorption constant is increased to fit the tracer residence time.

## 6.0 Comparison between the two models for prediction purposes

In this part of the report, the difference in the breakthrough curves predicted by means of the hydrodynamic dispersion model and the channeling dispersion model is shown. The two models give very similar results when fitted to experimental data for a non-sorbing tracer, but they describe different physical spreading mechanisms. So, if the parameters in both models, determined from a tracer test, are used to calculate breakthrough curves for other conditions, the resulting curves depend on the model selected.

For non-sorbing substances and short residence times the interaction with the granite matrix is negligible. When both models are used on given experimental data, a set of parameters is obtained:  $Pe$  and  $t_w$  for the hydrodynamic dispersion model and  $\sigma$  and  $\bar{t}_w$  for the channeling model. The curve forms differ only slightly and the fit is equally good with both models if measured as standard deviation of the fit.

When the breakthrough curve is predicted for the same fissure and flow distance but with a different water velocity, the results are independent of the selected model if - as is usually the case - the dispersion coefficient is assumed proportional to the water velocity. A different situation is obtained when the breakthrough curve is calculated for a fissure with equal properties but with a greater length. In this case the channeling dispersion model predicts a greater dispersion than the hydrodynamic dispersion model. Predicted breakthrough curves for a water velocity 10 times less and a length 10 times greater than the reference case are shown in figure 20. The difference between the curves is only due to the increase in fissure length. The Peclet number for the longer distance then is 100.

For the original fissure length  $\sigma = 0.21$  corresponds to  $Pe = 10$ . The assumptions inherent in the models are that  $\sigma$  is constant irrespective of length, in the channeling model, and  $D_L$  is independent of the length in the hydrodynamic dispersion model. An increase in length makes the Peclet number greater. It is proportional to the length,  $Pe = (U_f \cdot z) / D_L$ . As  $D_L$  is assumed to be proportional to the velocity, this does not influence Peclet number.

In experiments with non-sorbing and sorbing tracers, the data for the non-sorbing tracers may be used to determine the hydraulic properties ( $t_w$  and  $Pe$  or  $\sigma$ ). Using these parameters and the effective diffusivity and the sorption coefficients, breakthrough curves for the sorbing tracer may be predicted and compared with the experimental data. If only surface sorption is considered, the curves predicted using the channeling dispersion model show a slightly greater dispersion. In the smaller channels the surface retardation factor is greater than in the wider channels. Breakthrough curves for  $K_a$  value of  $4.0 \cdot 10^{-4}$  m are shown in figure 21. When the predictions are done for a greater distance the difference between both models is further increased. The channeling model shows significantly higher concentration at shorter times than the hydrodynamic dispersion model.

Breakthrough curves were also calculated considering surface sorption onto the fissure walls, diffusion into the rock matrix and sorption within the rock matrix. These curves are shown in figure 22 for a  $K_a$  value of  $1.0 \cdot 10^{-4}$  m and an interaction with the rock matrix corresponding to  $D_e \cdot K_d \cdot \rho_p = 1.0 \cdot 10^{-12}$  m<sup>2</sup>/s. The channeling dispersion model predicts a very much earlier arrival compared to the hydrodynamic dispersion model.

## 7.0 Discussion

The inlet concentration may be assumed to be known from the experimental conditions or may be determined by the fit. For the non-sorbing tracer no difference exists between them. The difference for the sorbing tracer test with strontium was about 15%. The inlet concentration determined in the fit was greater than the actual concentration in all cases. This indicates that there is some mechanism not accounted for in the models used. If the inlet concentration determined from the experiment is used, the agreement is poor. When the inlet concentration is determined by the fit the agreement is better, but the obtained inlet concentration is a little too high. The reason for this may be the existence of a greater porosity in the rock closest to the fissure. This has been noted experimentally in several samples (Skagius, 1984). The breakthrough curve would show a more pronounced interaction with the matrix for short times, when the tracer diffuses in zones with higher porosity. For longer times, when the tracer diffuses in zones with lower porosity, the interaction with the matrix is smaller and the breakthrough curve less influenced. Another reason for this difference may be due to the existence of a non-even flow through the fissure. The flow would be lower in the corner opposite the inlet and in the zone close to the flushing inlet (Eriksen, 1983).

The diffusion into the matrix and sorption within the rock matrix may be two important factors in the retardation of radionuclides (Neretnieks, 1980). To show the role of these mechanisms, the strontium tracer tests were fitted neglecting the interaction with the rock matrix. Only surface sorption and inlet concentration are determined.  $P_e$  and  $t_w$  were assumed to be known from non-sorbing tracer runs. The result for this fit is shown in figure 23, together with the fit including all the mechanisms. From the results it may be concluded that it is not possible to explain the behaviour of strontium in the fissure without considering the effects of matrix diffusion and sorption within the rock matrix. The impact of the diffusion into the rock matrix without sorption within the matrix is negligible. The fitted curve is similar to the curve where no diffusion into the rock is considered.



## 8.0 Conclusions

The hydrodynamic dispersion-diffusion model and the channeling dispersion-diffusion model used to analyse tracer tests performed in the laboratory both give good agreements.

For the non-sorbing tracers very similar results are obtained with both models. The relationship between the Peclet number and the standard deviation of the logarithmic fissure width distribution is very near to the expected value from the theoretical calculations.

The results for the sorbing tracer strontium are in fair agreement with the values determined in the laboratory for adsorption and matrix diffusion. The values obtained in the fit are to a certain extent dependent on the choice of the model. The fit with the hydrodynamic dispersion model gives a slightly smaller surface sorption coefficient and a higher interaction with the rock matrix than the fit using the channeling dispersion model.

The prediction of breakthrough curves for sorbing or non-sorbing tracer over longer distances is strongly dependent on the choice of model. The predicted breakthrough curves for longer distances using the channeling dispersion model show a higher dispersion and earlier arrival than the hydrodynamic dispersion model.

The distinction between the models cannot be made using experiments with the same migration distance.

## NOTATION

a	specific surface	$m^2/m^3$ fluid
A	parameter defined in eq. (9)	
B	parameter defined in eq. (14)	-
$C_f$	concentration in the liquid in the fissure	$mol/m^3$
$C_p$	concentration in the liquid in the pores	$mol/m^3$
$D_e$	effective diffusivity into the rock	$m^2/s$
$D_L$	dispersion coefficient	$m^2/s$
$K_a$	surface equilibrium coefficient	m
$K_d$	mass equilibrium coefficient	$m^3/kg$
Pe	Peclet number	
Q	flow rate	$m^3/s$
$R_a$	surface retardation factor in the channel	
s	standard deviation of the fit	
t	time	s
$t_0$	tracer residence time	s
$t_w$	water residence time	s
$U_f$	water velocity	m/s
x	distance in the direction of flow	m
z	distance into rock matrix	m
$\delta$	fissure width in the channel in the fissure	m
$\epsilon_p$	porosity of rock matrix	
$\lambda$	parameter defined in equation (6)	
$\mu$	mean of fissure width in the lognormal distribution	
$\rho_p$	density of rock matrix	$Kg/m^3$
$\sigma$	standard deviation in the lognormal distribution	

## REFERENCES

Carslaw, H.S. and Jaeger, J.C.: "Conduction of Heat in Solids". 2nd ed., Oxford University Press, New York (1959).

Eriksen, T.: "Radionuclide Transport in a Single Fissure. A Laboratory Study." KBS TR 83-01, Nuclear Fuel Safety Project, Stockholm (1983).

Levenspiel, O.: "Chemical Reaction Engineering", 2nd ed., Wiley International Ed., New York (1972).

Neretnieks, I.: "Diffusion in the Rock Matrix: An Important Factor in Radionuclide Retardation?" J. of Geophysical Res., Vol 85, 4379 (1980).

Neretnieks, I.: "A Note on Fracture Flow Mechanisms in the Ground", Water Resources Res., Vol 19, 364 (1983).

Neretnieks, I.; Eriksen, T. and Tähtinen, P.: "Tracer Movement in a Single Fissure in Granitic Rock: Some Experimental Results and Their Interpretation", Water Resources Res., Vol 18, 849 (1982).

Skagius, K. and Neretnieks, I.: "Diffusion in Crystalline Rocks of Some Sorbing and Nonsorbing Species." KBS TR 82-12, Nuclear Fuel Safety Project, Stockholm (1982).

Skagius, K. and Neretnieks, I.: "Diffusion Measurements in Crystalline Rocks." KBS TR 83-15, Nuclear Fuel Safety Project, Stockholm (1983).

Skagius, K.; Svedberg G. and Neretnieks, I.: "A Study of Strontium and Cesium Sorption on Granite". Nuclear Technology, Vol 59, 332 (1982).

Skagius, K.: Personal communication. Royal Institute of Technology (1984).

Snow, D.T.: "The Frequency and Apertures of Fractures in Rock". Int. J. Rock. Mech. Mil. Sci., vol. 7, 23 (1970).

Tang, G.H.; Frind, E.O. and Sudicky, E.A.: "Contaminant Transport in Fractured Porous Media. An Analytical Solution for a Single Fracture". Water Resources Res., Vol 17, 555 (1981).

Table 1

Experiments with non-sorbing substances. Curves fitted with the dispersion-diffusion model. Core A.

$$D_e = 0.1 \cdot 10^{-12} \text{ m}^2/\text{s}.$$

Run	Tracer	Peclet number Pe	Residence time $t_w$ min	Mean fissure width $\mu$ mm	Standard deviation of fit s/ $C_0$
A-1	NaLS	15.7	1.22	0.13	.01
A-2	NaLS	11.2	1.79	0.14	.01
A-3	NaLS	14.2	2.68	0.14	.04
A-4	NaLS	9.5	3.52	0.14	.03
A-5	NaLS	91.5	5.26	0.14	.02
A-6	NaLS	36.8	10.0	0.15	.02
A-7	NaLS	59.0	5.00	0.14	.01
A-8	NaLS	26.2	5.44	0.15	.03
A-9	NaLS	14.4	10.1	0.15	.02
A-10	NaLS	15.5	5.07	0.14	.01
A-11	3-H	109.0	2.99	0.16	.03
A-12	3-H	43.0	5.94	0.16	.03
A-13	3-H	85.2	11.9	0.17	.04
A-14	I	15.0	2.42	0.13	.02
A-15	Br	29.6	2.61	0.14	.01

Table 2

Experiments with non-sorbing substances. Curves fitted with the dispersion - diffusion model. Core B.

$$D_e = 0.1 \cdot 10^{-12} \text{ m}^2/\text{s}.$$

Run	Tracer	Peclet number Pe	Residence time $t_w$ min	Mean fissure width $\mu$ mm	Standard deviation of fit s/ $C_0$
B-1	NaLS	18.6	1.94	.14	.01
B-2	NaLS	9.9	2.24	.12	.02
B-3	NaLS	14.9	3.67	.12	.02
B-4	NaLS	80.2	4.56	.12	.01
B-5	NaLS	14.4	7.14	.13	.01
B-6	NaLS	13.2	15.3	.15	.02
B-7	3-H	15.8	4.55	.15	.01
B-8	3-H	48.2	8.97	.16	.02
B-9	3-H	40.0	18.1	.18	.03
B-10	I	9.5	4.07	.13	.03
B-11	Br	9.6	4.30	.14	.03

Table 3

Experiments with the sorbing substance strontium. Curves fitted with the hydrodynamic dispersion - diffusion model.

Run (1)	Tracer residence time $t_o$ min	A para- meter	Surface retarda- tion factor $R_a$	Surface sorption coeffic. (2)			Standard deviation of fit s/ $C_o$
				$\frac{C_o \text{ exp}}{C_o \text{ fit}}$	$K_a$ $10^5 \text{ m}$	$D_e K_d \rho_p$ $10^{12} \text{ m}^2/\text{s}$	
A-16	9.01	15.8	3.40	0.87	16.8	230	0.03
A-17	8.60	17.6	3.25	0.83	15.8	170	0.03
A-18	4.84	12.6	2.78	0.85	12.5	240	0.03
B-12	8.72	20.9	2.20	0.84	7.9	47	0.01
B-13	10.4	32.2	2.63	0.96	10.7	28	0.02
B-14	4.99	19.3	2.10	0.92	7.3	50	0.01

(1) The Peclet numbers are 20 for core A and 15 for core B.

(2)  $D_e K_d \rho_p$  determined in the laboratory is:

- $3.5 \cdot 10^{-12} \text{ m}^2/\text{s}$  for crushed granite particles
- $3.1 \cdot 10^{-12} \text{ m}^2/\text{s}$  for sawn pieces of granite.

Table 4

Experiments with non-sorbing substances. Experimental data fitted with the channeling dispersion model. Core A.

$D_e = 0.1 \cdot 10^{-12} \text{ m}^2/\text{s}$ . NaLS tracer.

Run	$\sigma$ for fissure width	Residence time $t_w$ min	Mean fissure width $\mu$ mm	Standard deviation of fit $s/C_0$
A-1	.176	1.27	.133	.01
A-2	.206	1.87	.151	.01
A-3	.186	2.79	.149	.03
A-4	.220	3.71	.150	.03
A-5	.055	5.32	.130	.02
A-6	.119	10.2	.148	.02
A-7	.096	5.08	.124	.02
A-8	.138	5.57	.151	.03
A-9	.180	10.5	.152	.02
A-10	.181	5.30	.130	.01



Table 5

Experiments with the sorbing tracer strontium. Experimental data fitted with the channeling dispersion model. Comparison with the hydrodynamic dispersion model.  $\sigma = 0.153$  in (1) and Pec = 20 in (2).

Run	Residence time $t_w$ min	Surface sorption coefficient		Surface sorption coefficient	
		$B^{(1)}$ $10^5$	$K_a^{(1)}$ $10^5$ m	$B^{(2)}$ $10^5$	$K_a^{(2)}$ $10^5$ m
A-16	2.65	1.32	26.4	1.51	16.8
A-17	2.65	1.15	23.7	1.29	15.8
A-18	1.74	1.39	19.5	1.54	12.5

(1) Values fitted with the channeling dispersion model.

$$B = (D_e K_d \rho_p)^{1/2}$$

(2) Values fitted with the hydrodynamic dispersion model.

$$B = \frac{\delta R_a}{2 A}$$

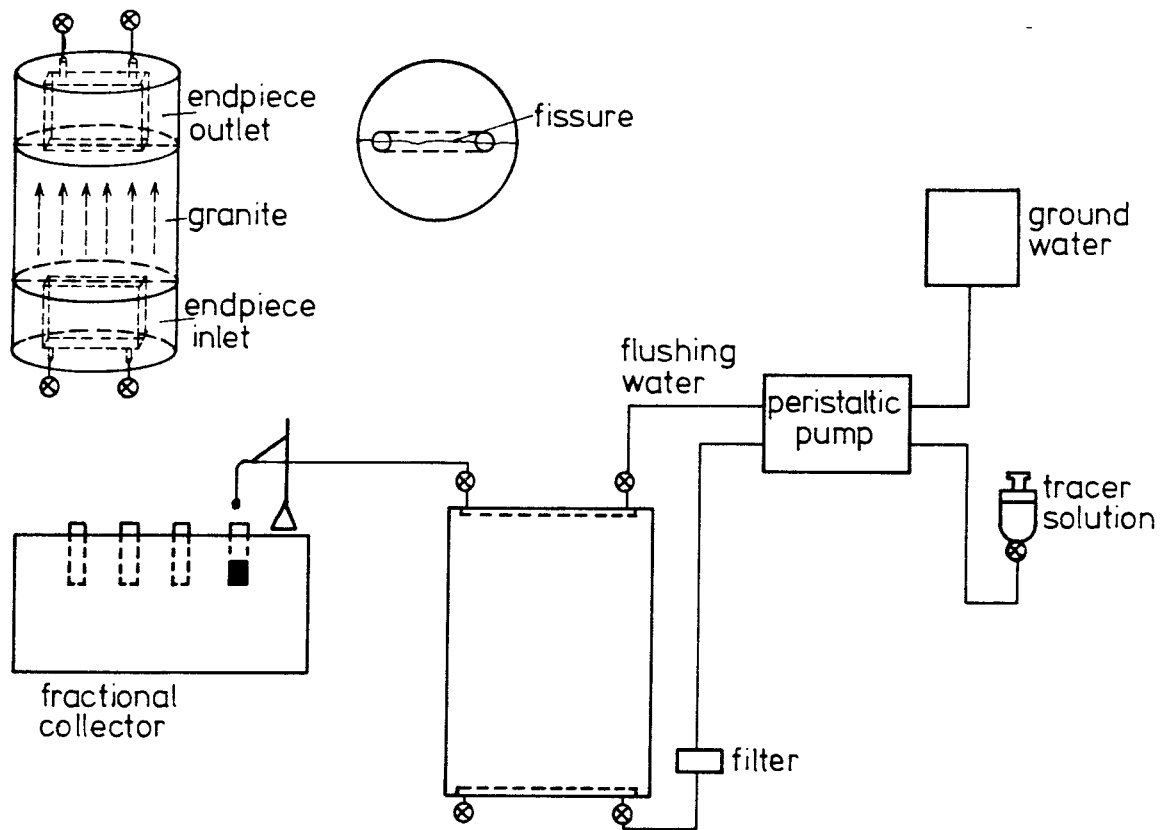


Figure 1. Experimental set up.

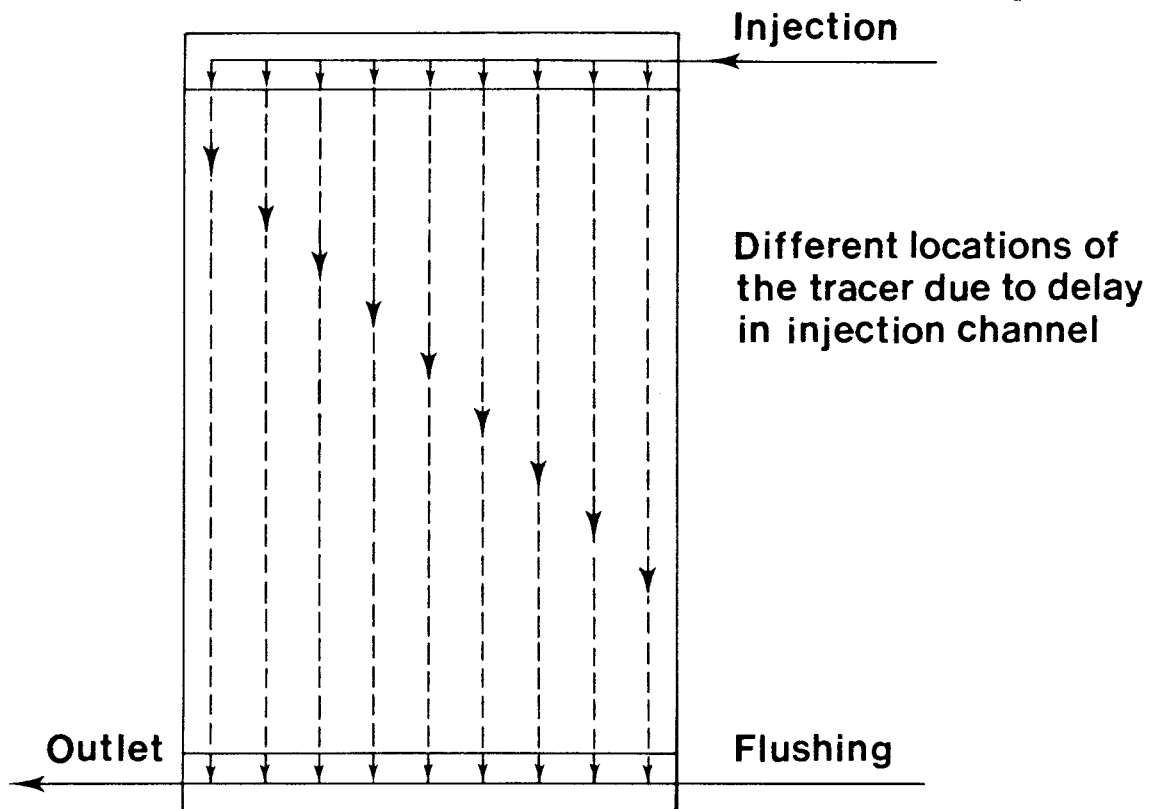
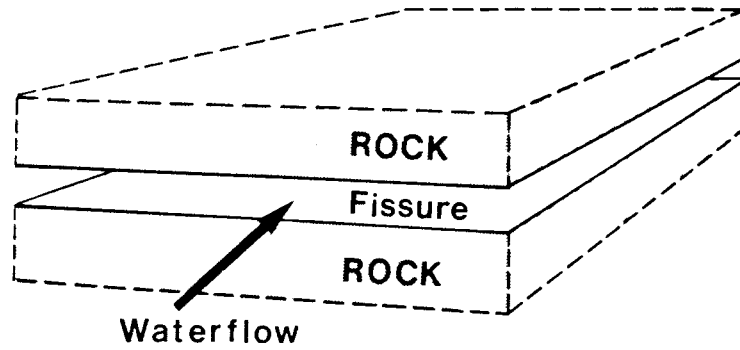
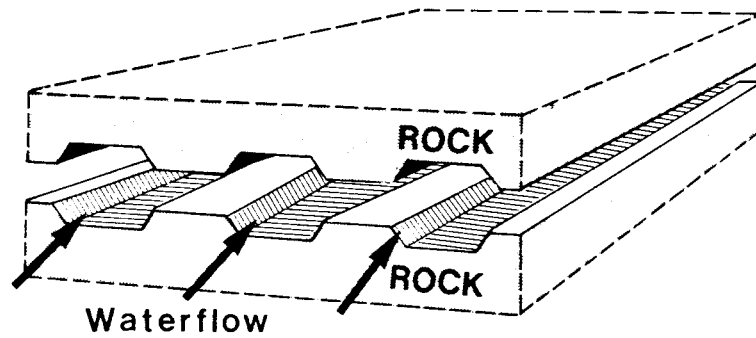


Figure 2a. The residence time distributions in inlet and outlet channels are accounted for in the model.



Same velocity and hydrodynamic dispersion in all channels.

Figure 2b. Hydrodynamic dispersion - diffusion model



Different velocities in different pathways. No dispersion.

Figure 2c. Channeling dispersion - diffusion model

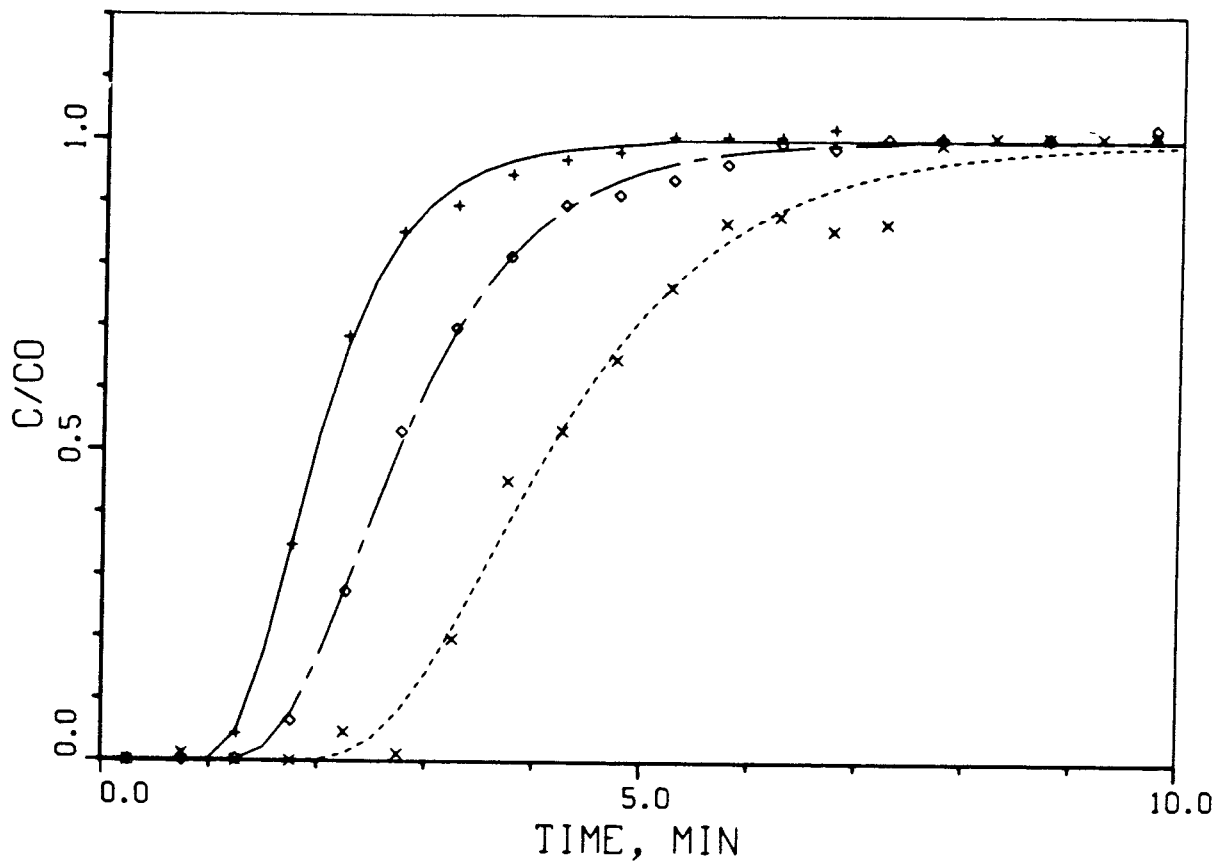


Figure 3. Curves fitted with the hydrodynamic dispersion model for non-sorbing tracers. Runs A1, A2, A3.

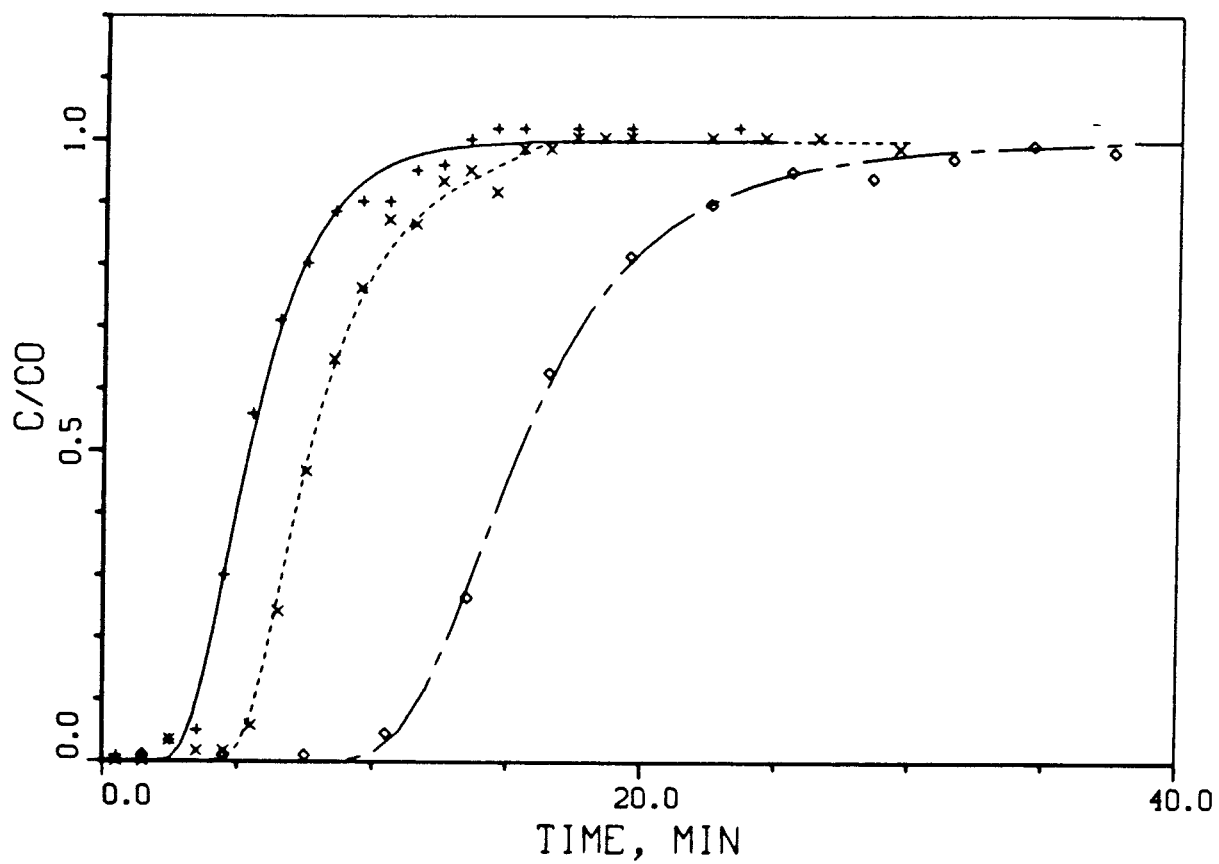


Figure 4. Curves fitted with the hydrodynamic dispersion model for non-sorbing tracers. Runs A4, A5, A6.

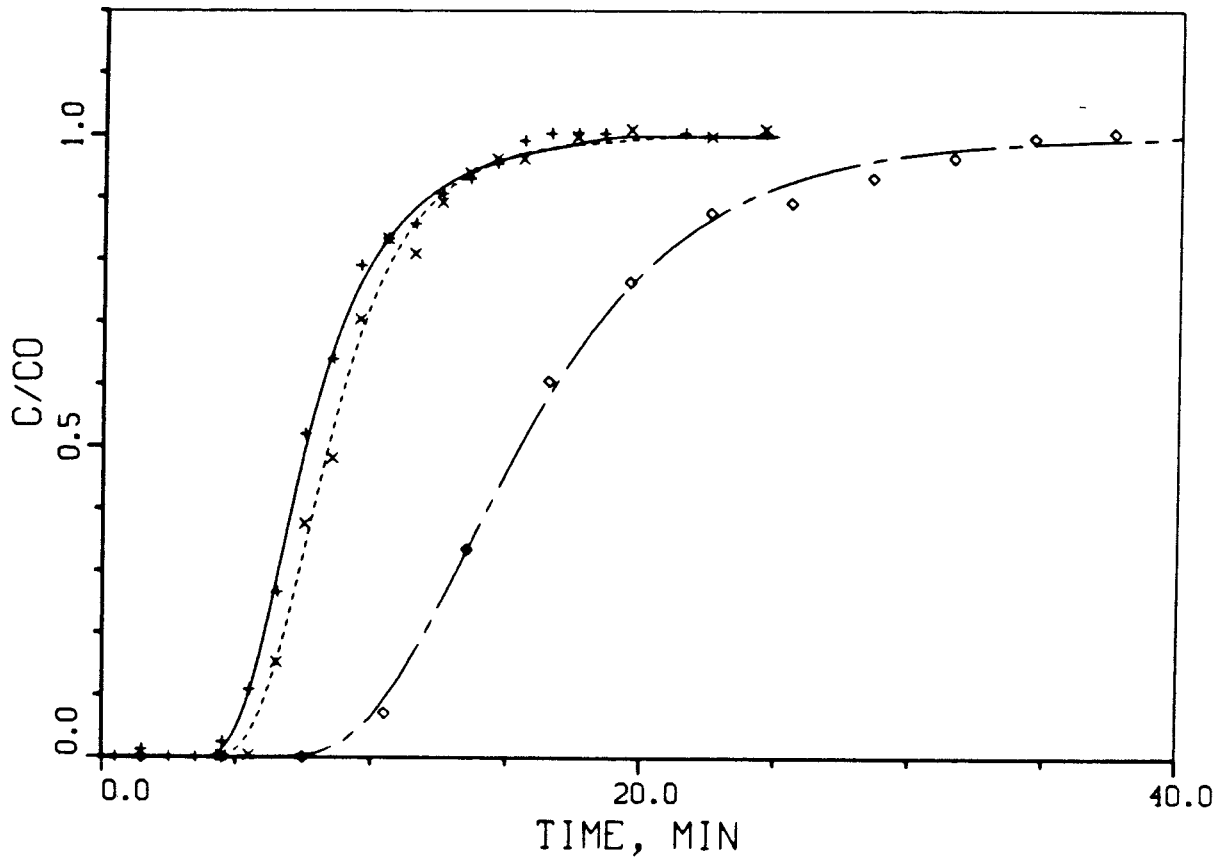


Figure 5. Curves fitted with the hydrodynamic dispersion model for non-sorbing tracers. Runs A7, A8, A9.

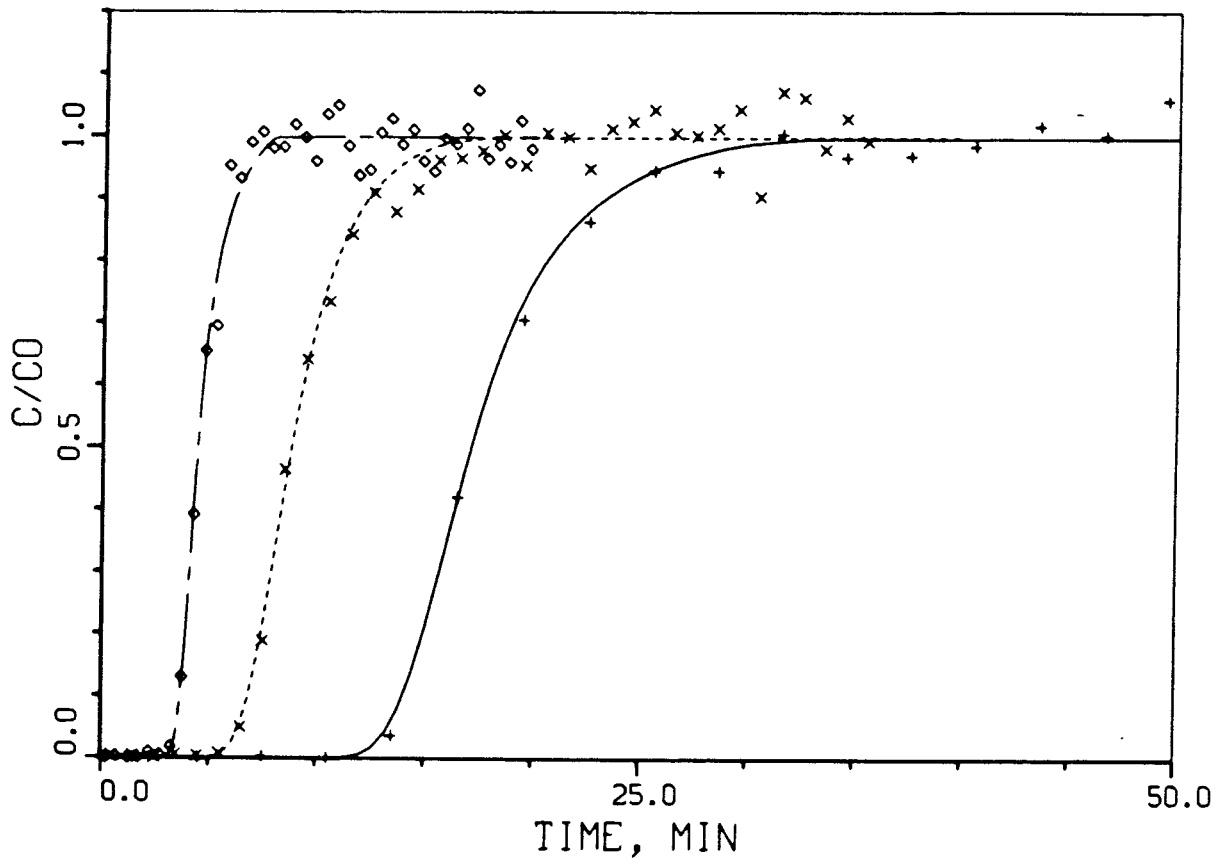


Figure 6. Curves fitted with the hydrodynamic dispersion model for non-sorbing tracers. Runs A11, A12, A13.



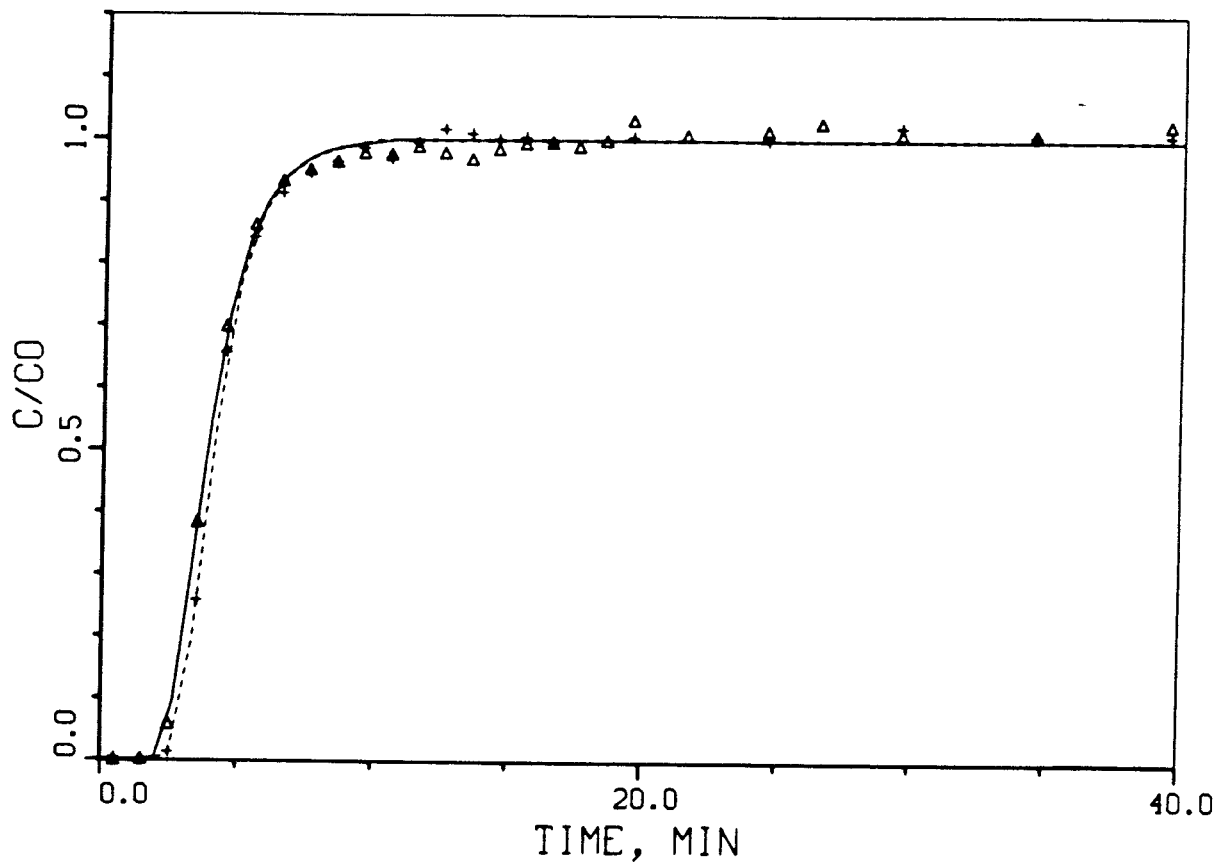


Figure 7. Curves fitted with the hydrodynamic dispersion model for non-sorbing tracers. Runs A14, A15.

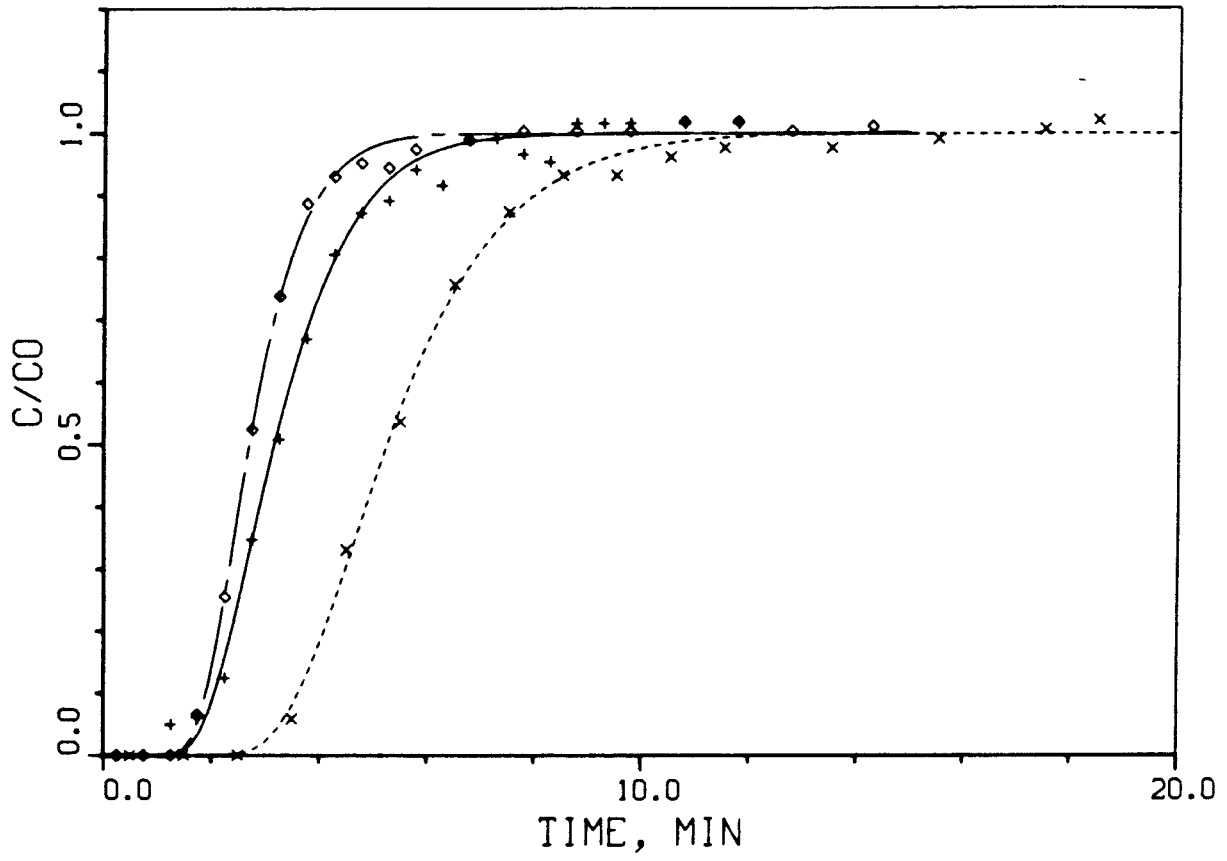


Figure 8. Curves fitted with the hydrodynamic dispersion model for non-sorbing tracers. Runs B1, B2, B3.

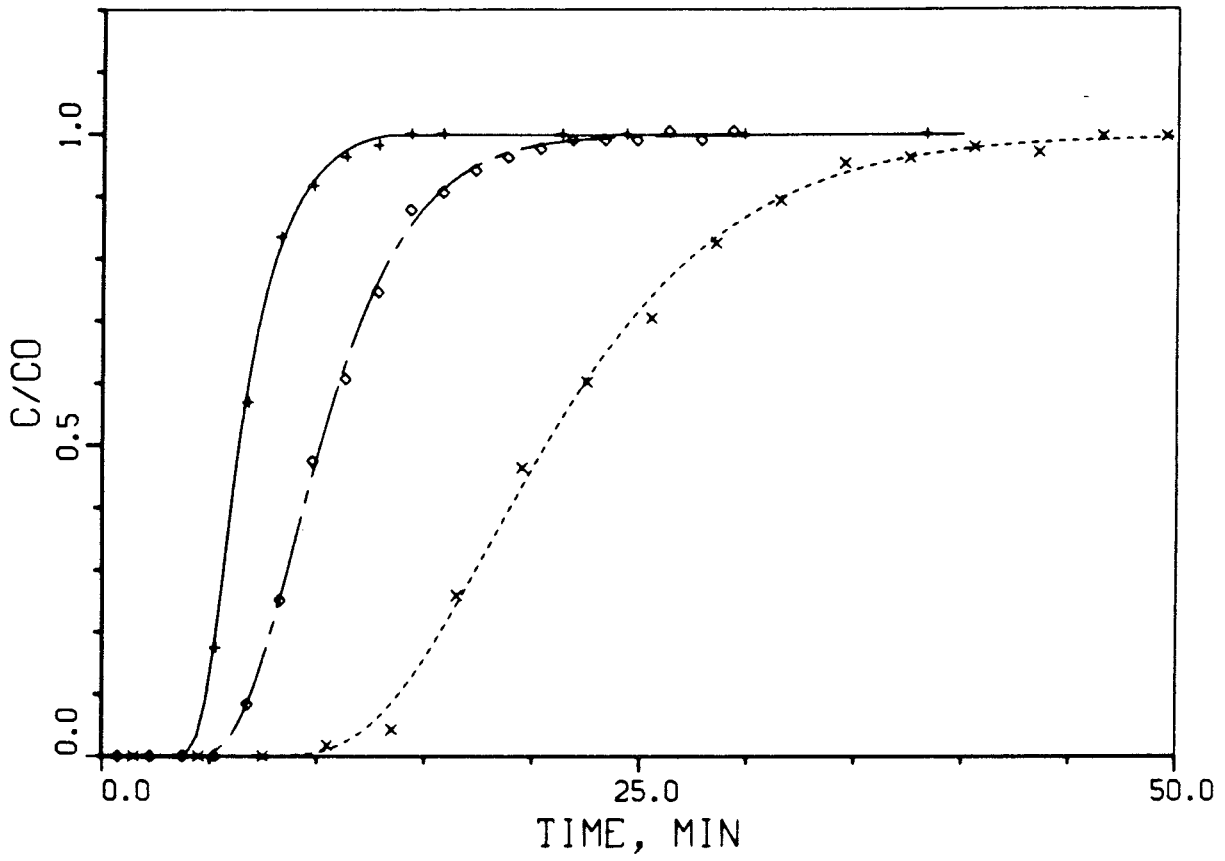


Figure 9. Curves fitted with the hydrodynamic dispersion model for non-sorbing tracers. Runs B4, B5, B6.

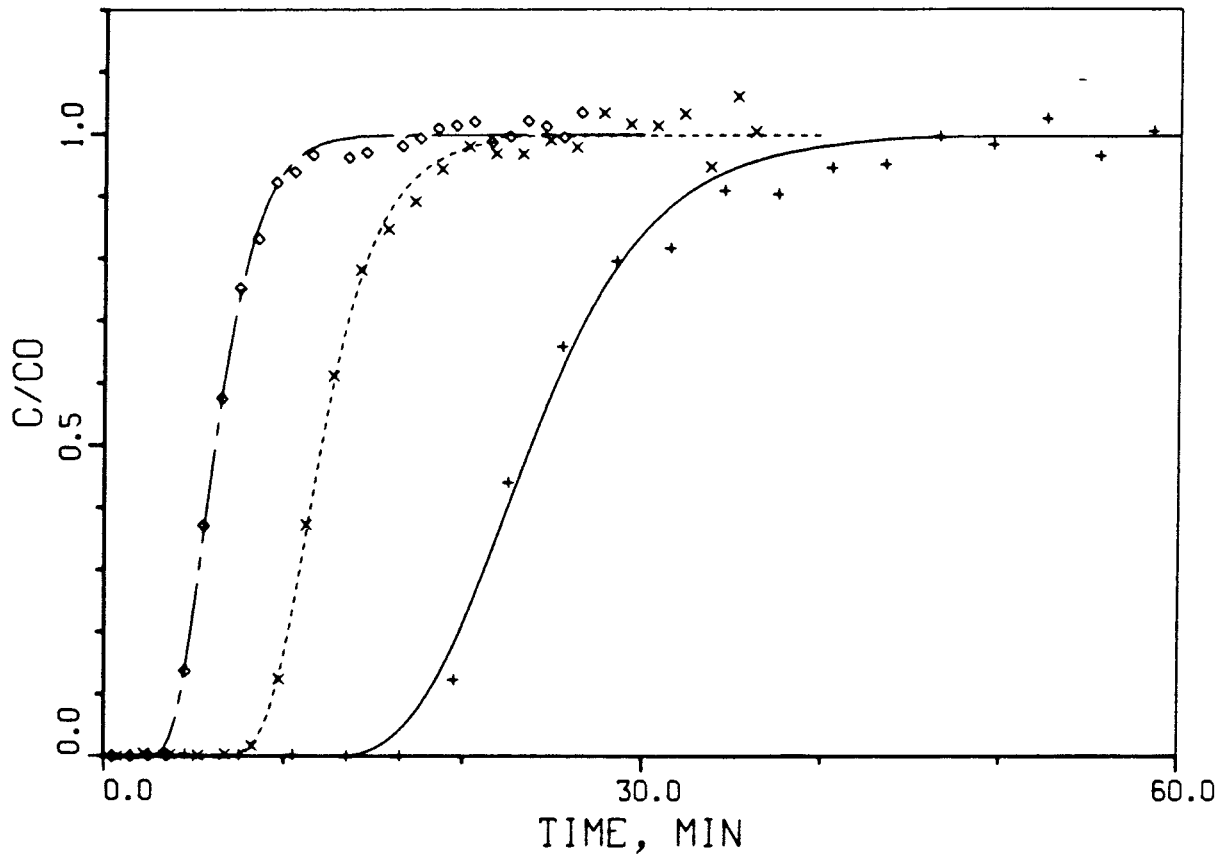


Figure 10. Curves fitted with the hydrodynamic dispersion model for non-sorbing tracers. Runs B7, B8, B9.

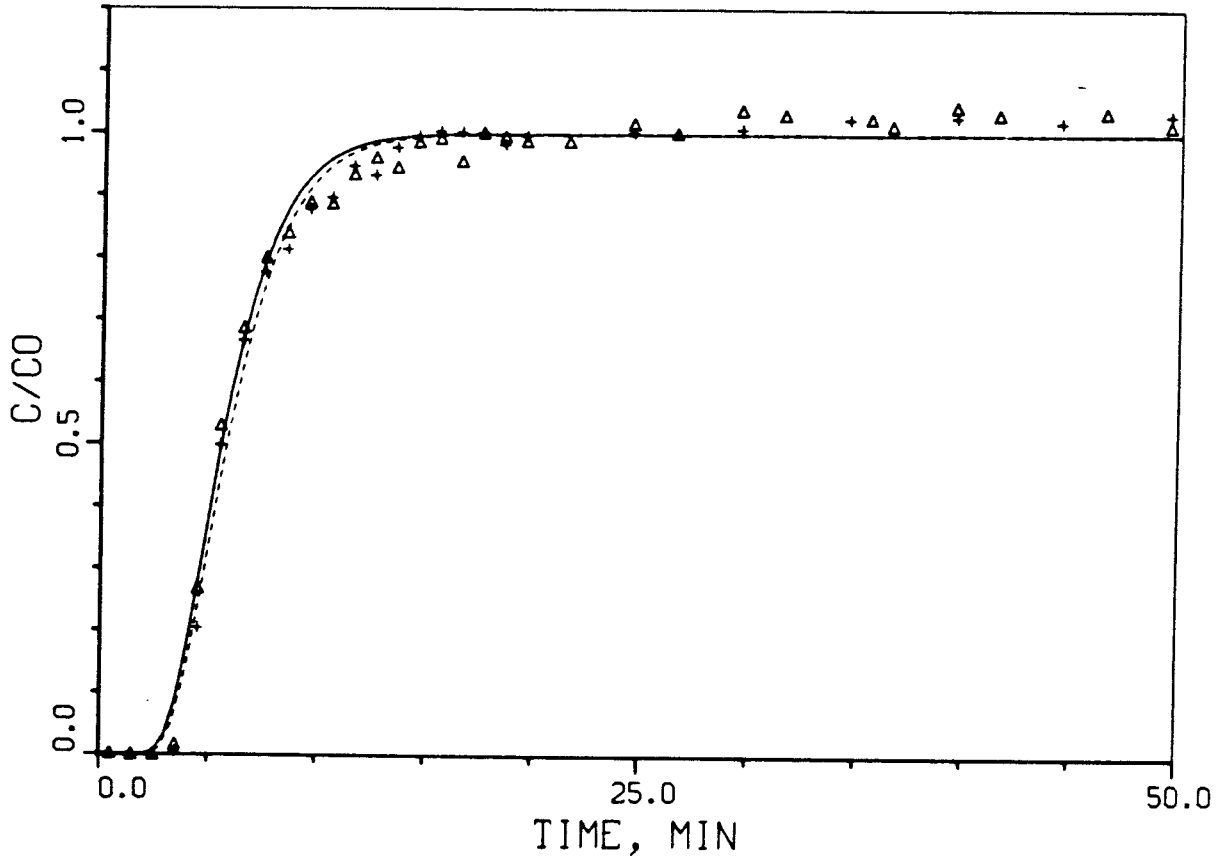


Figure 11. Curves fitted with the hydrodynamic dispersion model for non-sorbing tracers. Runs B10, B11.

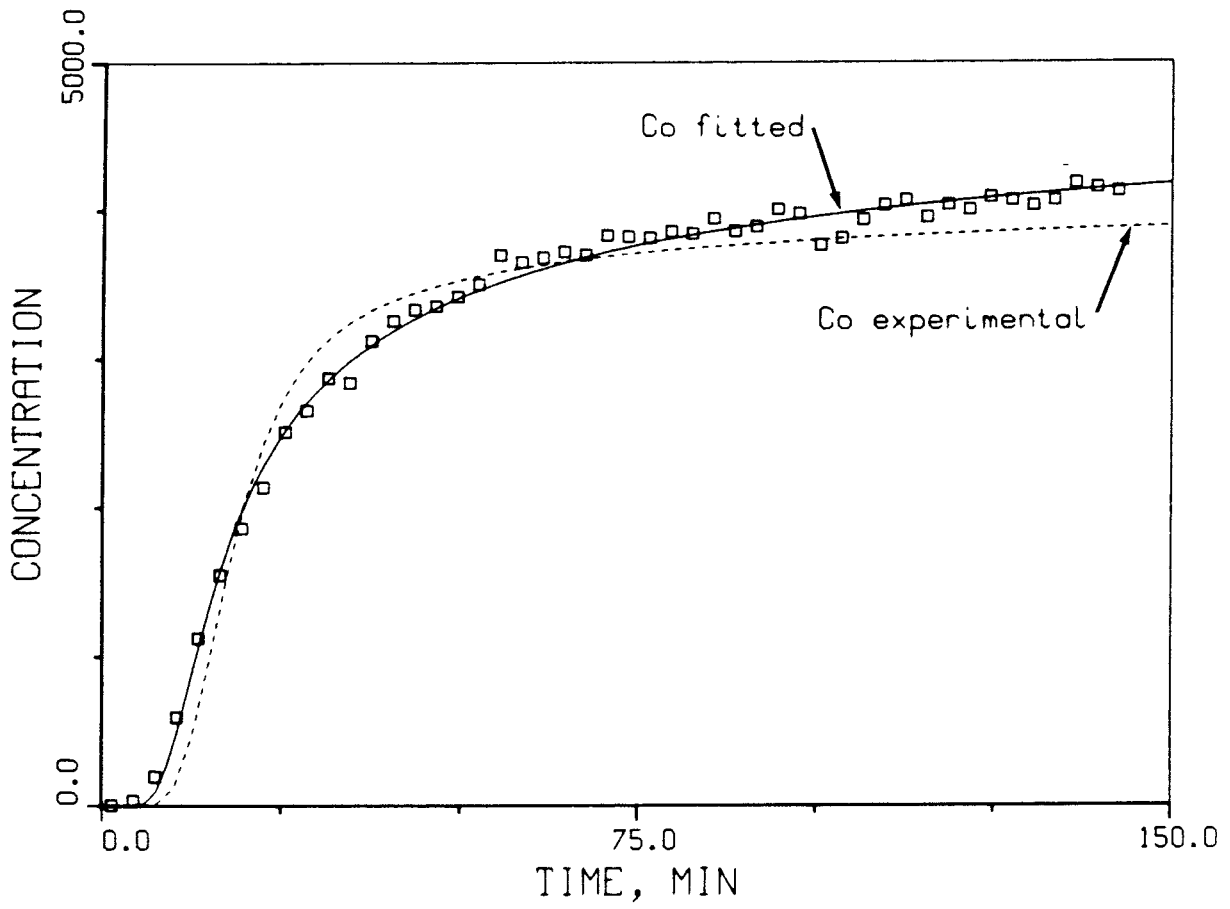


Figure 12. Curves fitted with the hydrodynamic dispersion model for strontium run A17. The reference concentration  $C_0$  is taken from experiments or included in the fit.

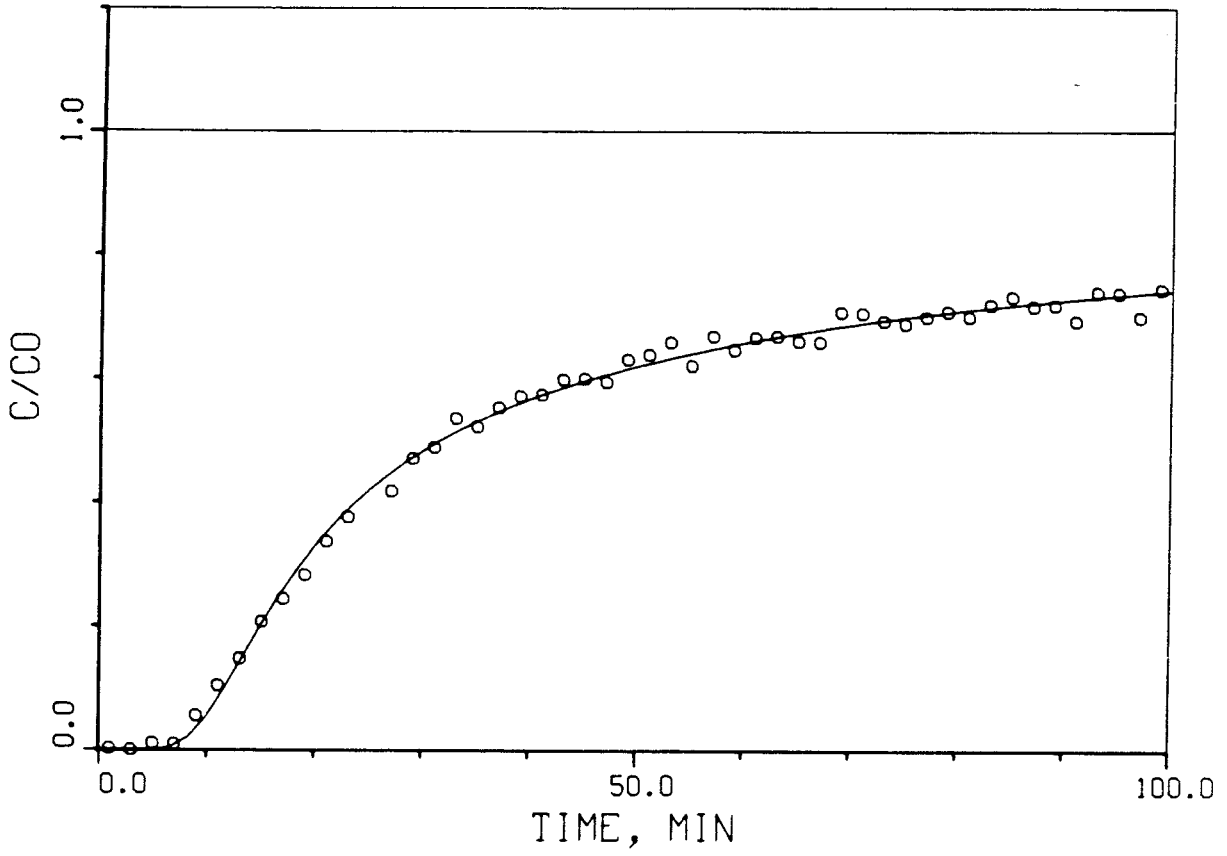


Figure 13. Curve fitted with the hydrodynamic dispersion model for strontium. Run A16,  $C_0$  fitted.

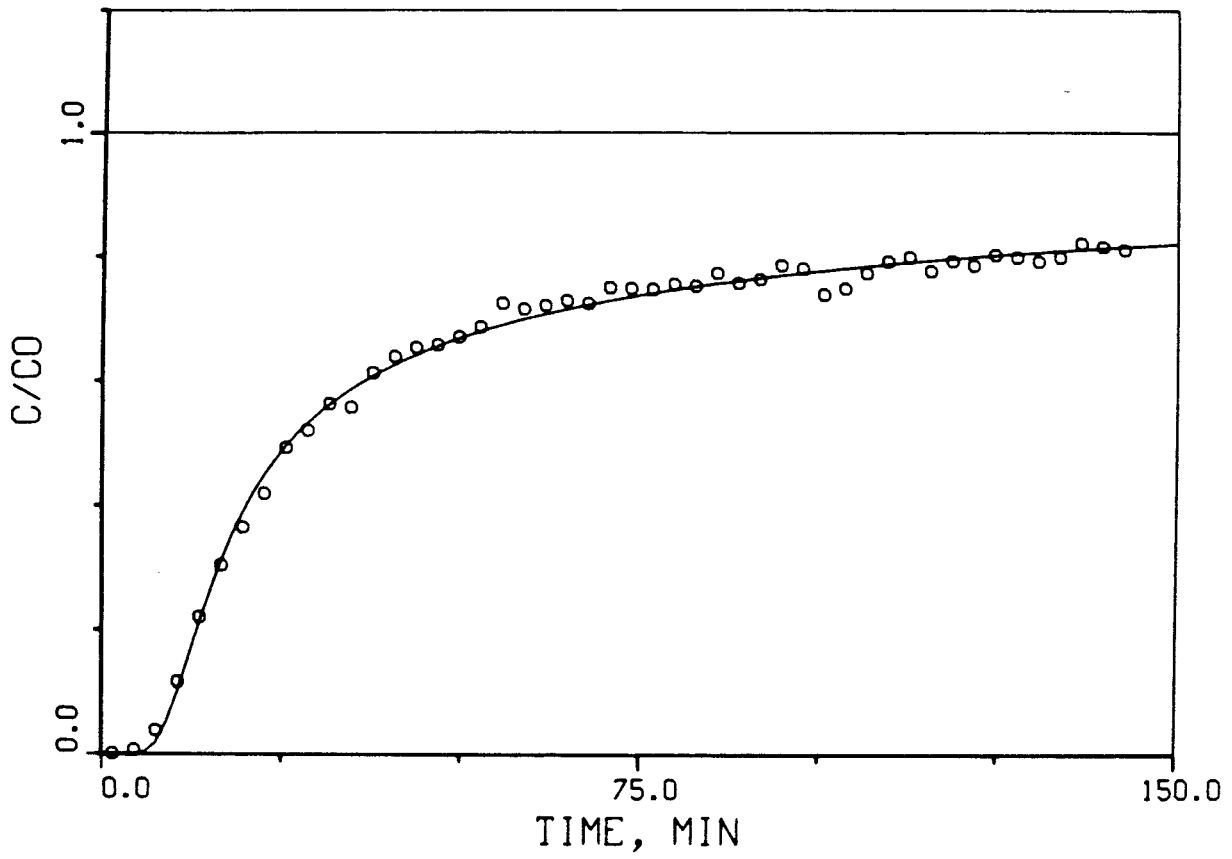


Figure 14. Curve fitted with the hydrodynamic dispersion model for strontium. Run A17,  $C_0$  fitted.



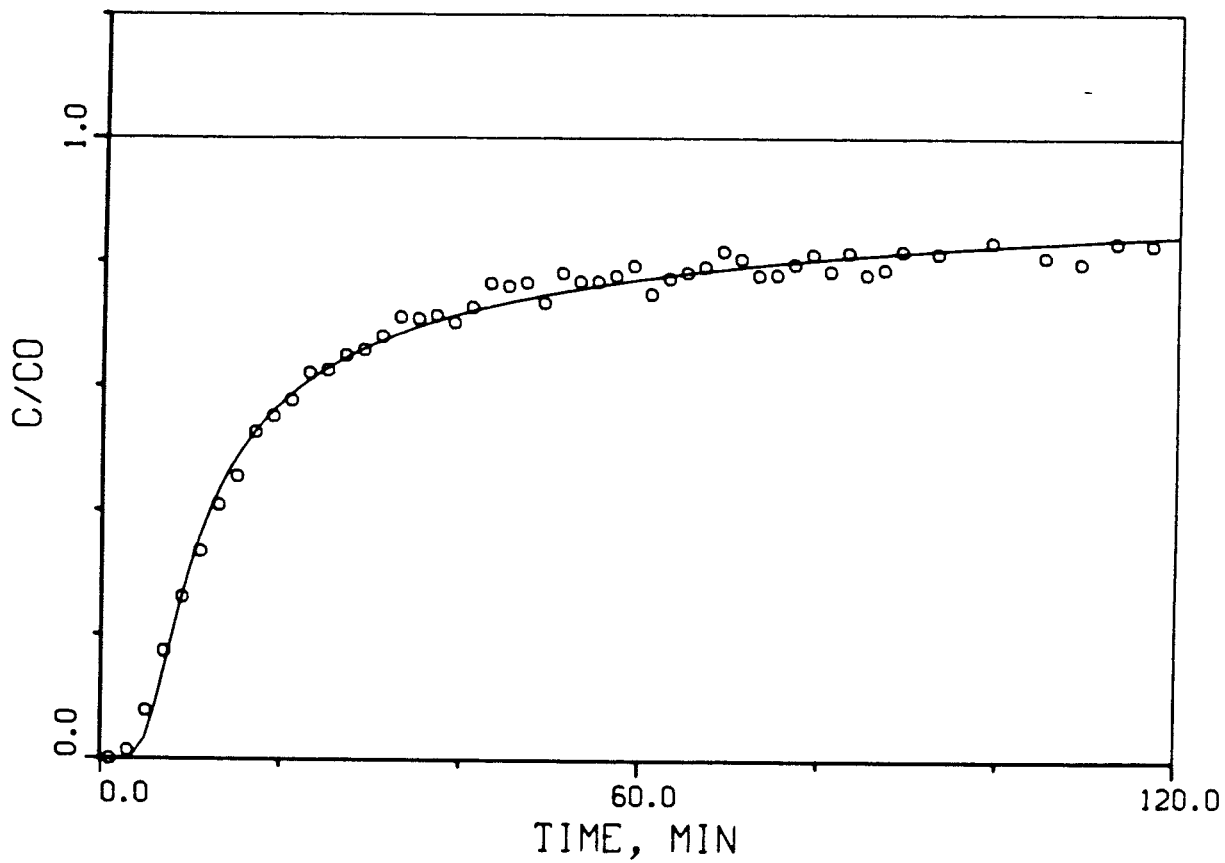


Figure 15. Curve fitted with the hydrodynamic dispersion model for strontium. Run A18,  $C_0$  fitted.

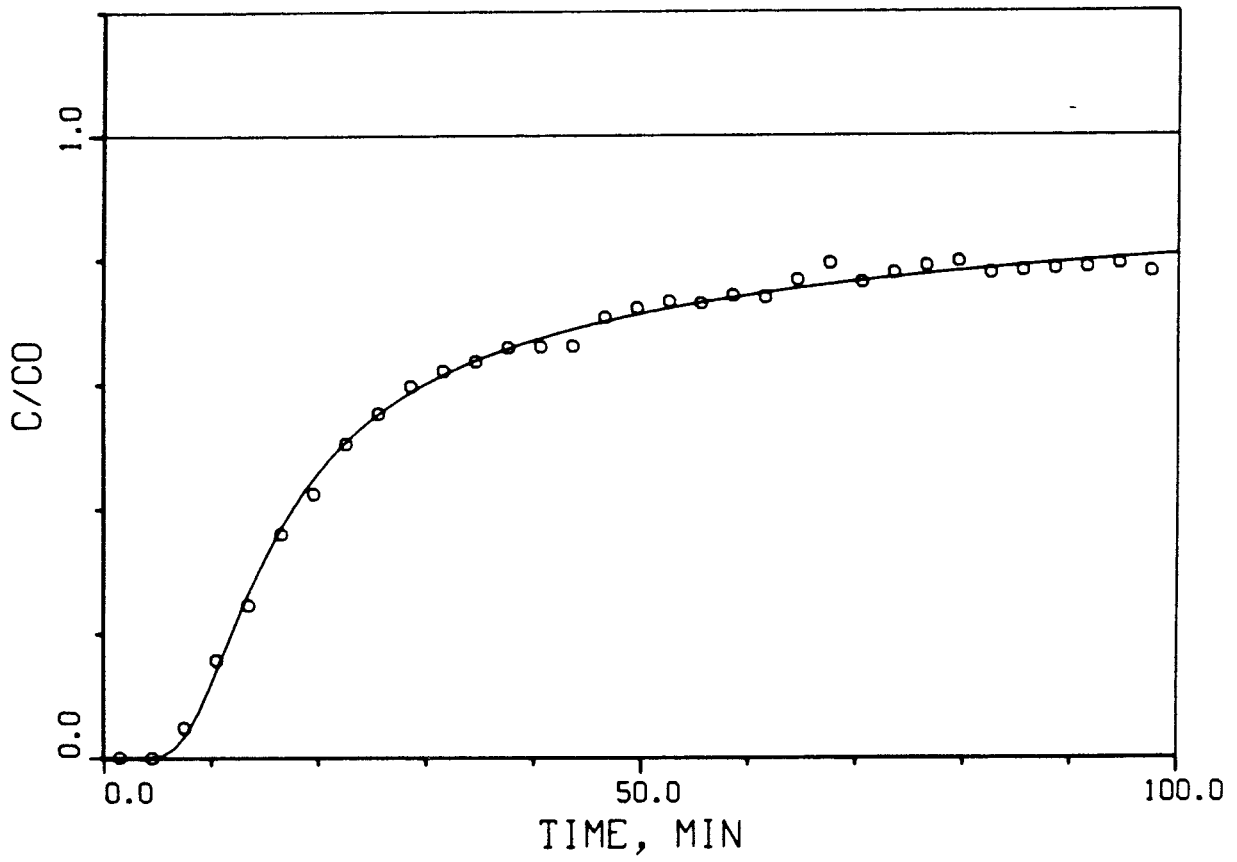


Figure 16. Curve fitted with the hydrodynamic dispersion model for strontium. Run B12,  $C_0$  fitted.

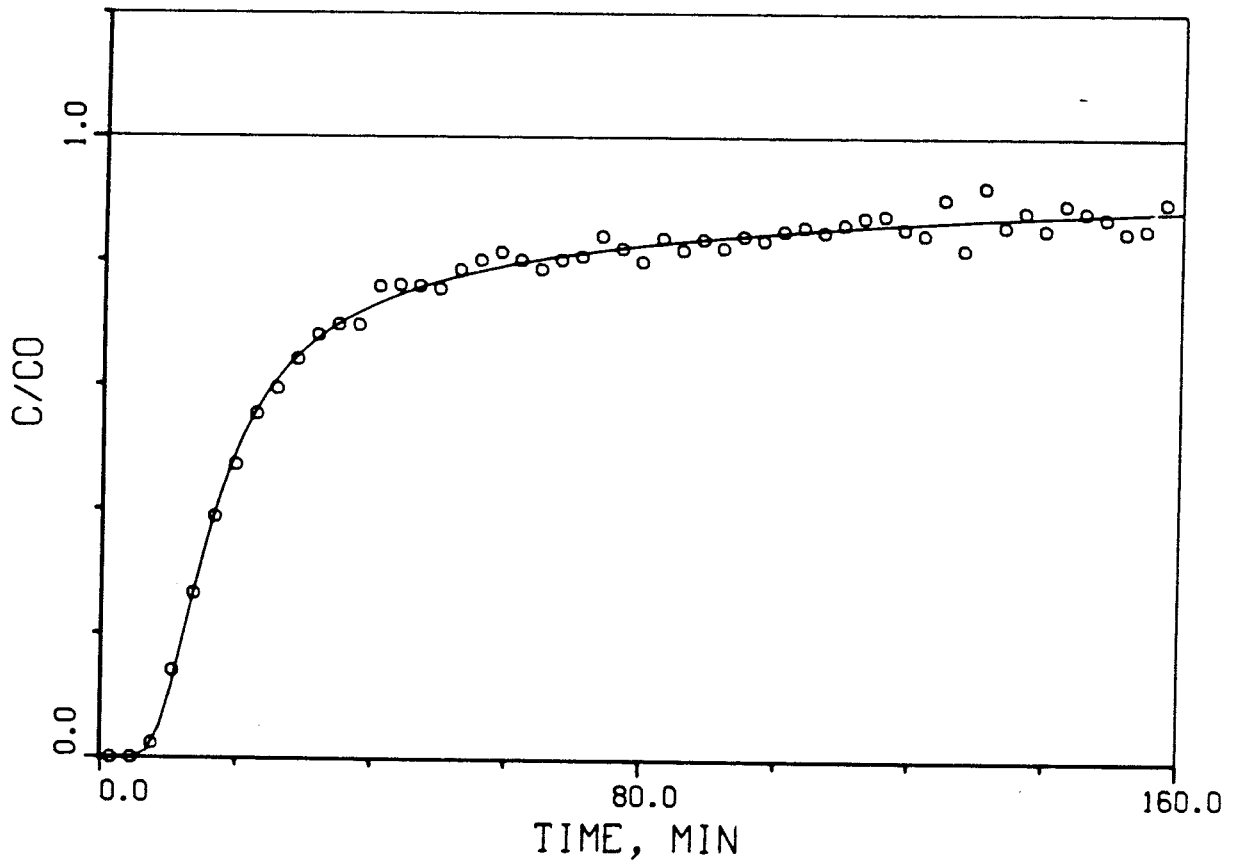


Figure 17. Curve fitted with the hydrodynamic dispersion model for strontium. Run B13,  $C_0$  fitted.

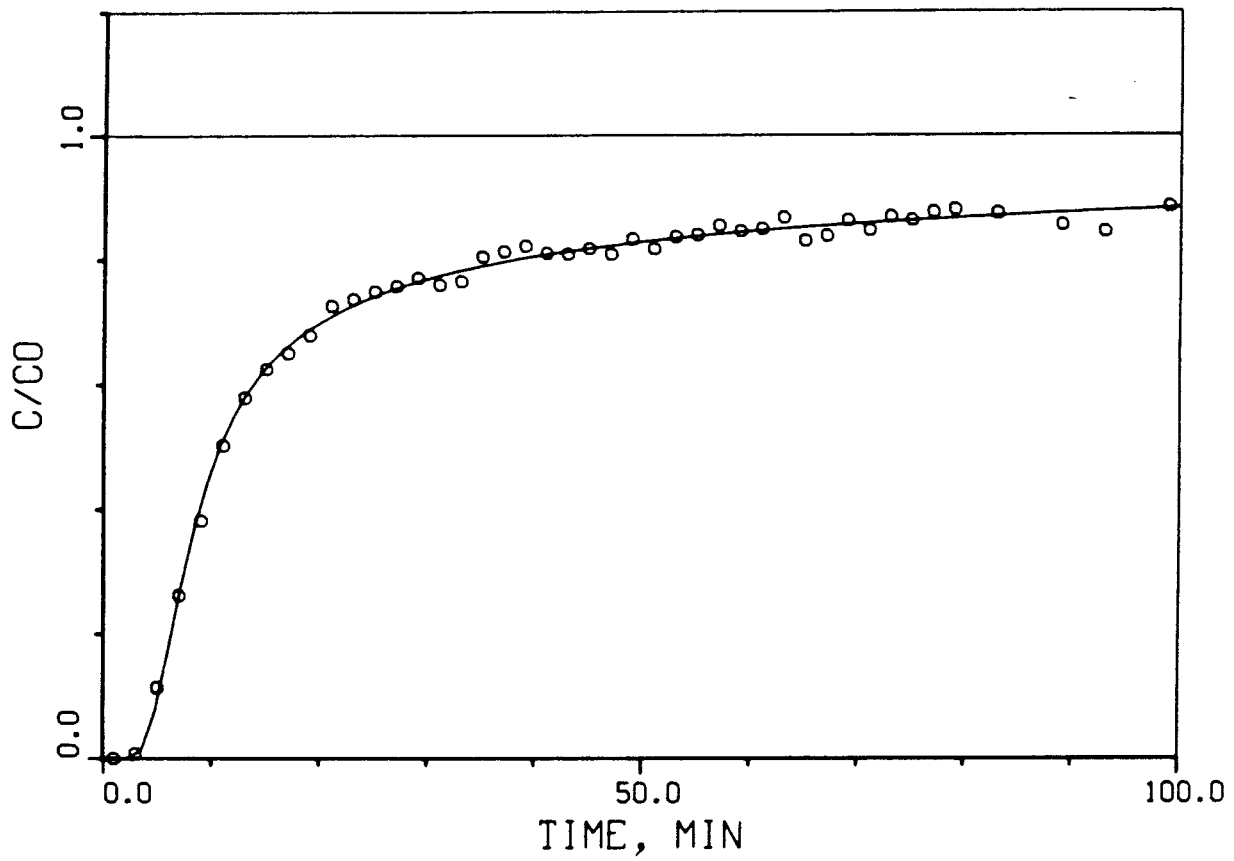


Figure 18. Curve fitted with the hydrodynamic dispersion model for strontium. Run B14,  $C_0$  fitted.

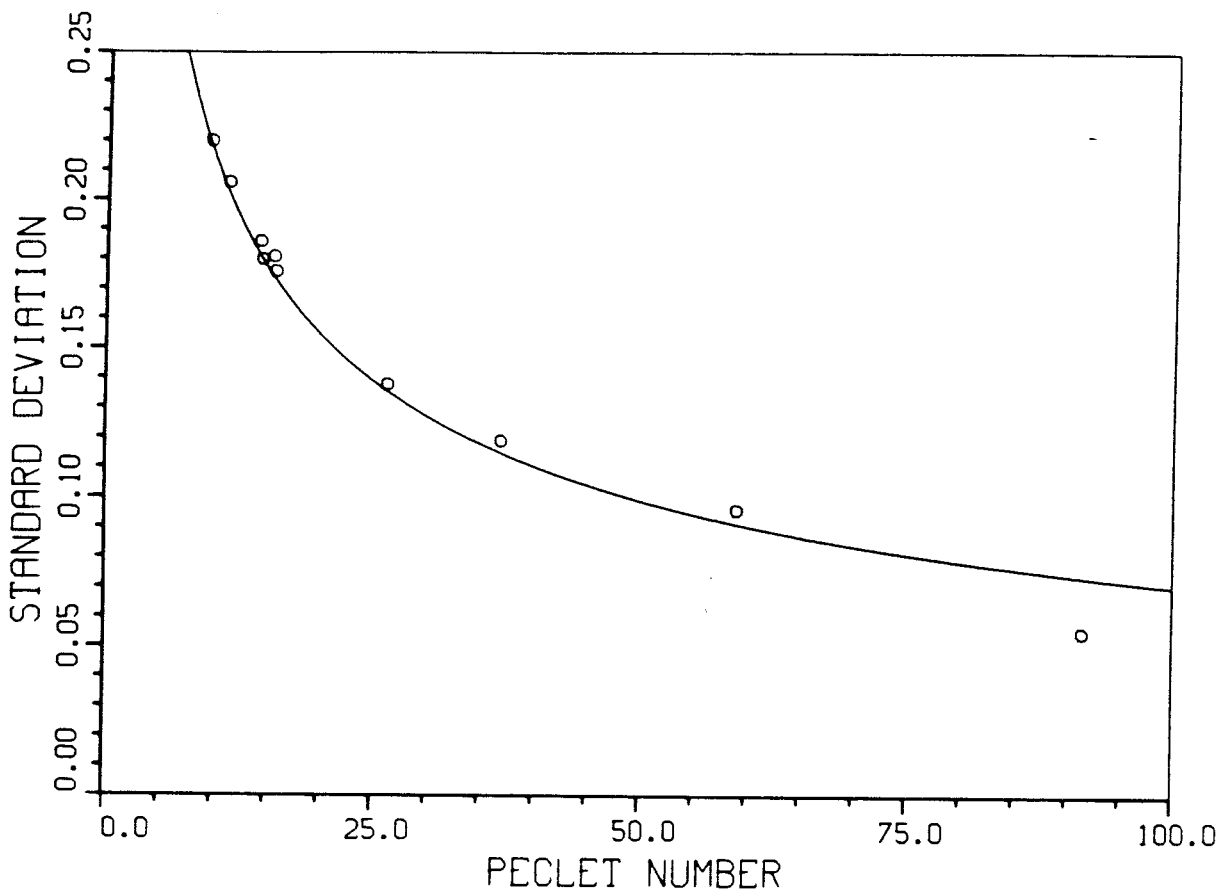


Figure 19. Relationship between Peclet number and standard deviation of the logarithm of the fissure width.

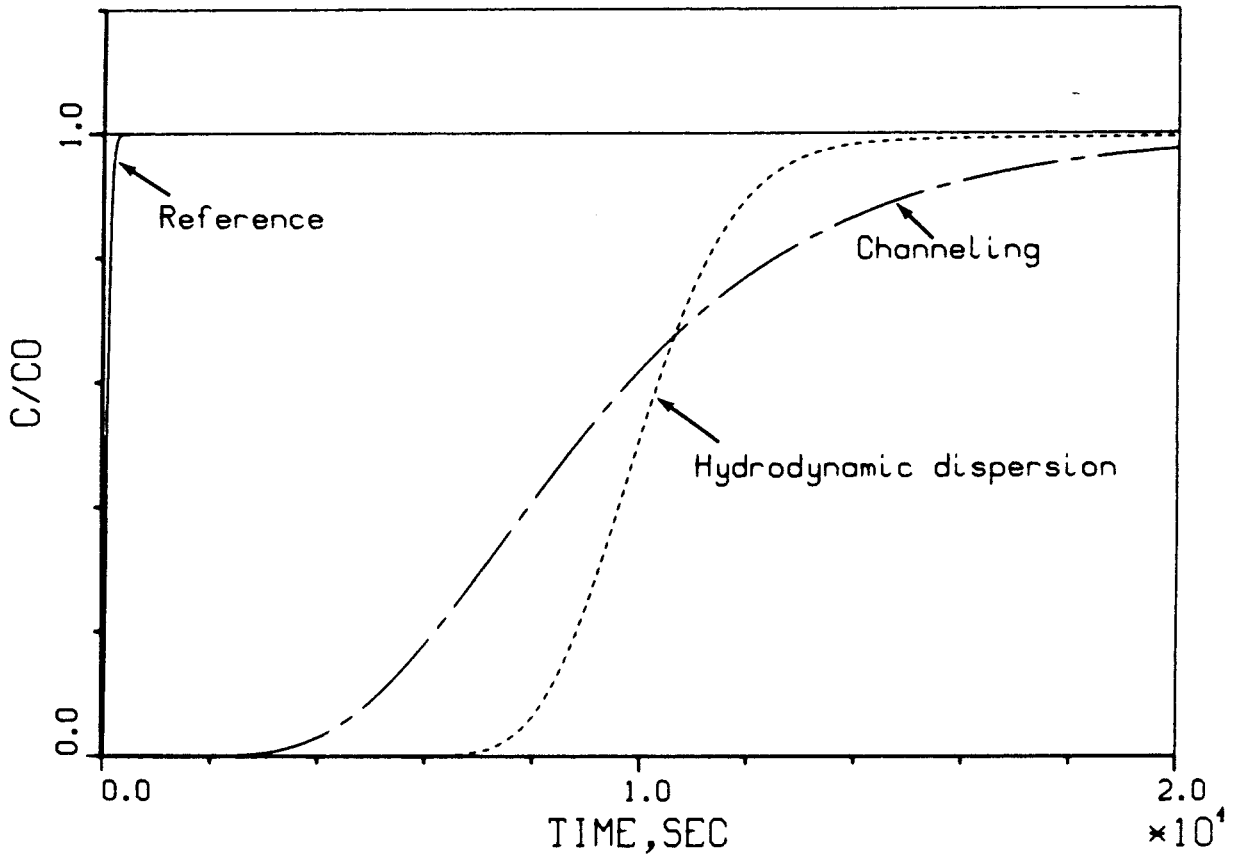


Figure 20. Predicted curves using the hydrodynamic dispersion model and the channeling dispersion model. For non-sorbing tracer for a longer distance (10 times) and a lower flow. ( $Pe = 100$ ,  $\sigma = 0.208$ )

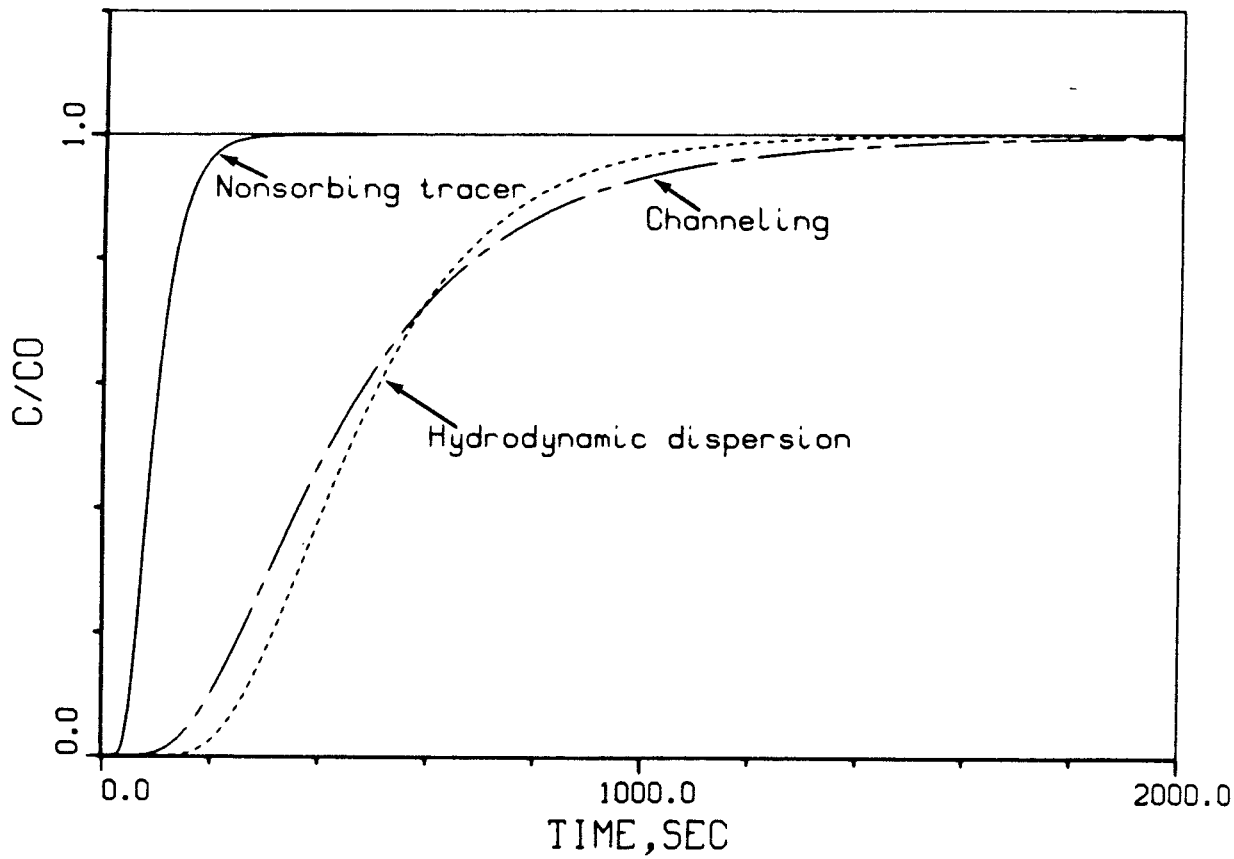


Figure 21. Predicted curves using the hydrodynamic dispersion model and the channeling dispersion model. For sorbing tracer assuming only surface sorption. ( $Pe = 10$ ,  $\sigma = 0.208$ ,  $K_a = 4 \cdot 10^{-4}$  m, this gives  $R_a = 5$  for the hydrodynamic dispersion model)

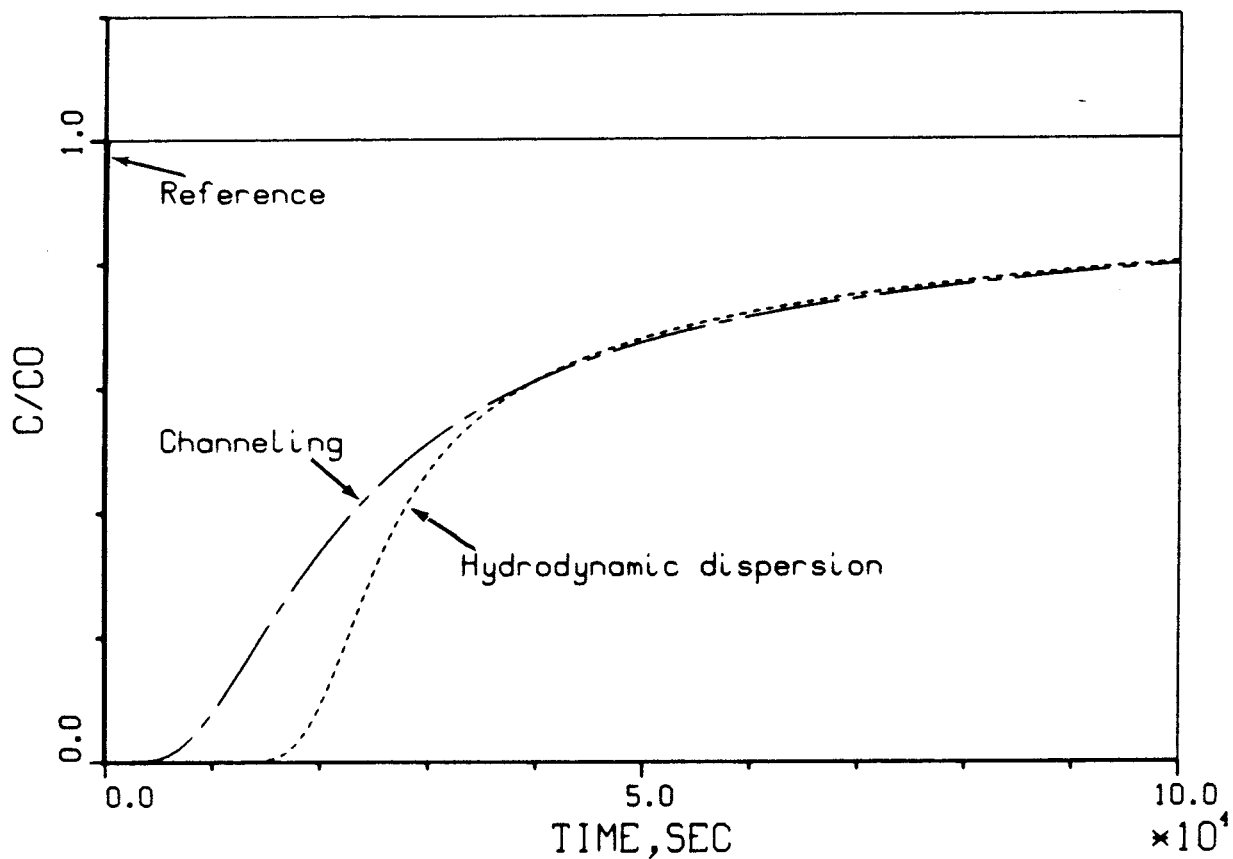


Figure 22. Predicted curves using the hydrodynamic dispersion model and the channeling dispersion model. For sorbing tracer considering surface and volume sorption and diffusion into the matrix and for a longer distance and lower flow. ( $Pe = 100$ ,  $\sigma = 0.208$ ,  $D_e \cdot K_d \cdot \rho_p = 1.0 \cdot 10^{-12} \text{ m}^2/\text{s}$ ,  $K_a = 1 \cdot 10^{-4} \text{ m}$ )



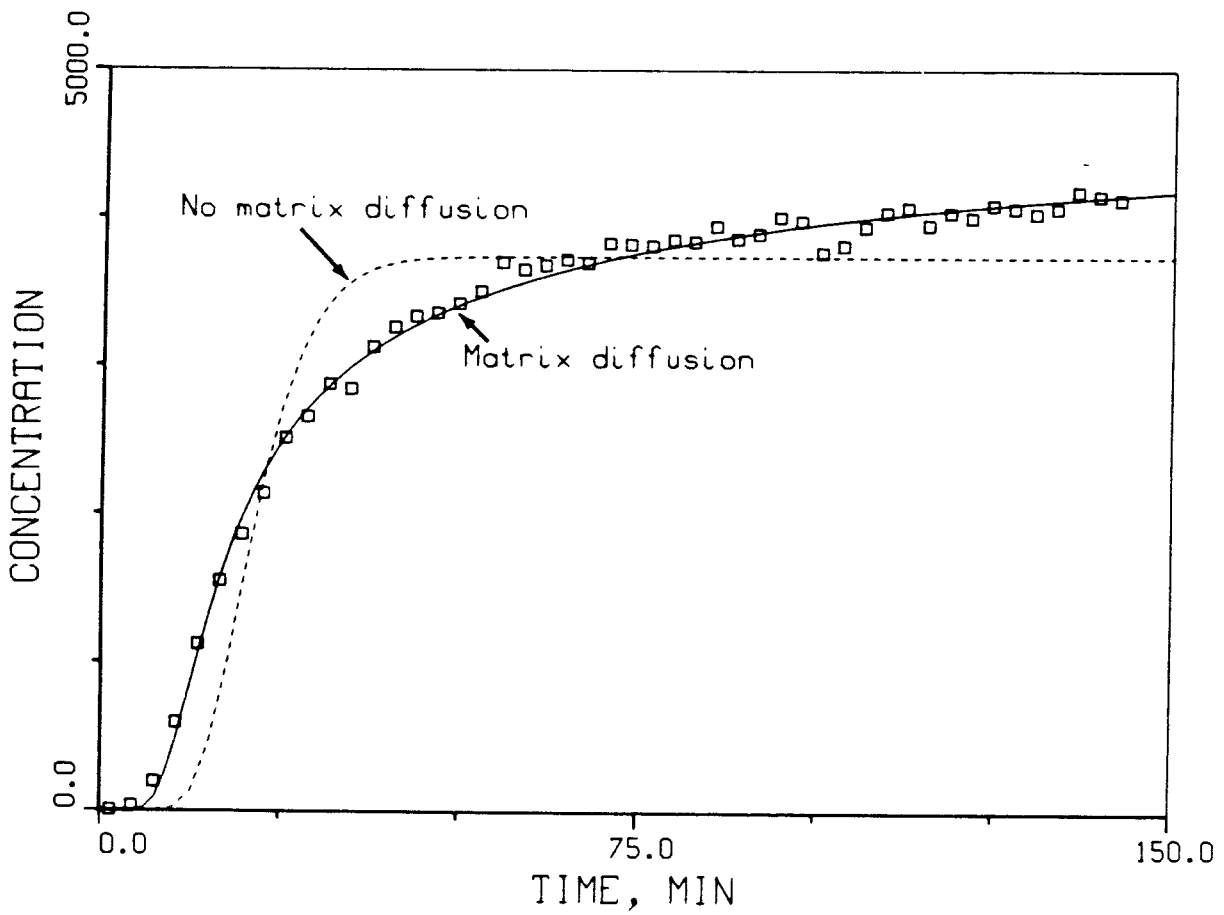


Figure 23. Curve fitted using the Hydrodynamic dispersion model for sorbing tracer. With and without matrix diffusion. In both cases  $Pe$  from non-sorbing tests were used. ( $Pe = 20$ )

# *List of KBS's Technical Reports*

1977–78

TR 121

**KBS Technical Reports 1 – 120.**

Summaries. Stockholm, May 1979.

1979

TR 79–28

**The KBS Annual Report 1979.**

KBS Technical Reports 79-01 – 79-27.

Summaries. Stockholm, March 1980.

1980

TR 80–26

**The KBS Annual Report 1980.**

KBS Technical Reports 80-01 – 80-25.

Summaries. Stockholm, March 1981.

1981

TR 81–17

**The KBS Annual Report 1981.**

KBS Technical Reports 81-01 – 81-16.

Summaries. Stockholm, April 1982.

1982

TR 82–28

**The KBS Annual Report 1982.**

KBS Technical Reports 82-01 – 82-27.

1983

TR 83–77

**The KBS Annual Report 1983.**

**KBS Technical Reports 83-01–83-76**

**Summaries. Stockholm, June 1984.**

1984

TR 84–01

**Radionuclide transport in a single fissure**

**A laboratory study of Am, Np and Tc**

Trygve E Eriksen

Royal Institute of Technology

Stockholm, Sweden 1984-01-20

TR 84-02

**Radiolysis of concrete**

Hilbert Christensen

Studsvik Energiteknik AB,

Nyköping, Sweden

Erling Bjergbakke

Risö National Laboratory,

Roskilde, Denmark 1984-03-16

TR 84-03

**Effect of  $\beta$ -radiolysis on the products from**

**$\alpha$ -radiolysis of ground water**

Hilbert Christensen

Studsvik Energiteknik AB,

Nyköping, Sweden

Erling Bjergbakke

Risö National Laboratory

Roskilde, Denmark

1984-07-10